Climatic Origin of Dm-Scale Compositional Cyclicity in the Upper Devonian Cleveland Member of the Ohio Shale, Central Appalachian Basin

Jacek Jaminski[1,*], Thomas J. Algeo[1],
J. Barry Maynard[1], and James C. Hower[2,3]

[1]H. N. Fisk Laboratory of Sedimentology
Department of Geology
University of Cincinnati
Cincinnati, OH 45221-0013

*Present address:
Amoco Exploration & Production
P.O. Box 3092
Houston, TX 77253-3092

[2]Center for Applied Energy Research
3572 Iron Works Pike
Lexington, KY 40511-8433

[3]Department of Geological Sciences
University of Kentucky
Lexington, KY 40506-0059

(In: Algeo, T.J., and Maynard, J.B. (Eds.), 1997. *Cyclic Sedimentation of Appalachian Devonian and Midcontinent Pennsylvanian Black Shales: Analysis of Ancient Anoxic Marine Systems—A Combined Core and Field Workshop*: Joint Meeting of Eastern Section AAPG and The Society for Organic Petrography (TSOP), Lexington, Kentucky, Sept. 27-28, 1997, p. 26-62.)

ABSTRACT

High-frequency variation in environmental conditions within the anoxic Late Devonian Appalachian Basin was investigated through microstratigraphic analysis of the Cleveland Member of the Ohio Shale in four cores from central Ohio and northern Kentucky. In each core, X-radiography revealed pervasive decimeter-scale compositional cyclicity, and selected cycles were sampled at a sub-centimeter scale to identify compositional controls on X-radiograph gray-scale density (GSD) values. Petrographic and geochemical analysis of samples revealed that (1) the main controls on GSD are total carbon (TC; a proxy for organic carbon) and total sulfur (TS; a proxy for Fe-sulfides), which account for roughly equal amounts of GSD variance, and (2) dm-scale cyclicity in GSD values represents compositional variation between a high TC-low TS and a low TC-high TS endmember, reflecting strong negative covariation between TC and TS at a decimeter scale. Further, (3) the high TC-low TS endmember contains large amounts of poorly-preserved (i.e., bacterially reworked) organic matter of probable marine algal origin, whereas the low TC-high TS endmember contains smaller quantities of well-preserved organic matter of mainly marine algal origin, and (4) the high TC-low TS endmember is enriched in trace elements associated with organics and a high-Ti-Zr detrital group (probably a silt-size clastic fraction), whereas the low TC-high TS endmember is enriched in trace elements associated with Fe-sulfides and a high-Al-K detrital group (probably a clay-size clastic fraction). The high TC-low TS endmember of dm-scale cycles may have been deposited at low bulk sedimentation rates, allowing bacterial reworking and concentration of organic matter, whereas the low TC-high TS endmember may have been deposited at high bulk sedimentation rates, resulting in better preservation of organic matter and in introduction of reactive Fe that promoted formation of authigenic Fe-sulfides. These inferences are consistent with a process model invoking accumulation of organic matter in a starved-basinal setting subject to fluctuations in freshwater runoff and in water- and wind-borne clastic fluxes as a result of climatic forcing at timescales of a few thousand years. An important conclusion of the present study is that analysis of laminated organic-rich sediments must be undertaken at length scales shorter than those of natural compositional variation in order to accurately characterize the depositional dynamics of anoxic marine systems.

INTRODUCTION

Preservation of primary compositional variation at a fine scale in anoxic marine environments commonly yields a laminated sedimentary record in which individual laminae record information regarding "instantaneous" environmental conditions and successions of laminae record changes in such conditions over extended intervals of time (Hay et al., 1990; Lyons, 1991; Peterson et al., 1991; Ripepe et al., 1991; Aplin et al., 1992). Knowledge of environmental conditions at a given moment in time, and of changes in such conditions over short time intervals, is invaluable in understanding depositional and early diagenetic processes that control the accumulation of sedimentary organic matter. Although analysis of such controls optimally would entail generation and evaluation of high-frequency compositional records over long stratigraphic intervals at a number of locales within a sedimentary basin, geochemical analysis of compositional variation in laminated sediments is labor-intensive. As a consequence, most geochemical studies of ancient organic-rich sediments (i.e., black shales) have resorted either (1) to wide sample spacing (e.g., Leventhal, 1981; Robl et al., 1983; Beier and Hayes, 1989; Ripley et al., 1990) or (2) to a limited stratigraphic and geographic scope of investigation (e.g., Ingall et al., 1993). Although the former approach provides information about long-term environmental changes, it runs the risk of overlooking signals at a frequency higher than that represented by mean sample spacing or of recognizing spurious signals at the limit of spatial resolution of the data (a process known as "aliasing" in time series analysis). On the other hand, the latter approach may fail to identify significant patterns of environmental variation at longer timescales or over broader areas.

In order to efficiently characterize fine-scale compositional variation in laminated organic-rich sediments over extended stratigraphic intervals, we have developed a combination of techniques that utilizes X-radiography as a primary tool. Our procedure entails (1) generation of X-radiographs over the complete stratigraphic interval of interest in laminated sedimentary cores, providing a continuous high-resolution record of density variations that serve as a geochemical proxy (Algeo et al., 1994), and (2) detailed petrographic and geochemical analysis of selected short core intervals for identification of compositional controls on density variation. To date, we have utilized this procedure to study sub-mm-scale compositional variation over stratigraphic intervals of tens of meters in a number of black shale formations of Middle Ordovician to Early Permian age. In this report, we will focus on results from the Upper Devonian Cleveland Member of the Ohio Shale, which was studied in four cores from Ohio and Kentucky (Fig. 1; Jaminski et al., 1995). X-radiographic, petrographic, and geochemical data of the present study were integrated with existing stratigraphic and paleoclimatic reports for the Late Devonian Appalachian Basin (e.g., Potter et al., 1980; de Witt and Roen, 1985; Woodrow, 1985; Ettensohn et al., 1989; Roen and Kepferle, 1993) to allow evaluation of environmental variation from a lamina scale to a basinal scale and construction of a depositional model for controls on the accumulation of sedimentary organic matter.

CHOICE OF STUDY UNITS

The Cleveland Member of the Ohio Shale (henceforth: Cleveland Shale) is a black, organic carbon-rich unit that is approximately correlative with the Late Devonian (late Famennian) *expansa* conodont zone (Fig. 2A; Woodrow et al., 1988; Ziegler and Sandberg 1990). In Ohio and Kentucky, the Cleveland Shale exhibits evidence of dm-scale compositional variation in the form of a ribbed weathering pattern in outcrop (Potter et al., 1982). Weak color variation (olive-black to brownish-black) is apparent at similar length scales in some cores, but quantifying such subtle color changes would be difficult, e.g., using optical microdensitometry, a method that has been applied successfully to limestone-shale successions exhibiting strong color contrast (Herbert and Fischer, 1986; Bond et al., 1992). Despite minimal color variation, the ribbed weathering pattern of the Cleveland Shale is a reflection of strong dm-scale compositional variation, primarily with regard to concentrations of organic matter (4-14 wt% TOC) and sulfides (1-6 wt% TS). Owing to differences in density between organic carbon, sulfides, and the silicate matrix, X-radiography is capable of imaging spatial variation in the distribution of these components and of providing a high-resolution proxy record of compositional variation.

In order to examine geographic as well as stratigraphic patterns of fine-scale compositional variation in the Cleveland Shale, a series of four cores was chosen between central Ohio and northern Kentucky, representing a gradient from more proximal (northern) to more distal (southern) environments (Fig. 1). These cores are located on the eastern flank of the Cincinnati Arch (i.e., west of the depocenter of the Appalachian Basin), which is a favorable location for analysis of fine-scale compositional variation in Appalachian Devonian black shales because of (1) isolation from sources of coarse clastic influx, such as the Catskill Delta, on the northern and eastern margins of the basin (Craft and Bridge, 1987), and (2) relative completeness of the Upper Devonian stratigraphic succession, compared with condensed sections of stratigraphic equivalents to the south, such as the upper Gassaway Member of the Chattanooga Shale (Schieber, 1994). Owing to space limitations, the present paper will focus on X-radiographic, petrographic, and geochemical data from a single core (OHRS-5 from Ross County, Ohio; Fig. 1), but the reader should note that the depositional model presented in the final section of this paper is based on evaluation of stratigraphic and geochemical data from all four study cores.

In southern Ohio, the Cleveland Member of the Ohio Shale is part of a thick succession of Upper Devonian black shales that includes the Huron Member of the Ohio Shale and the Sunbury Shale (Fig. 2A). These organic-rich units were deposited under moderately deep-water, starved-basinal conditions that were interrupted by episodic influx of coarser clastics, such as the Bedford-Berea sequence (Ettensohn and Elam, 1985; Pashin and Ettensohn, 1995). To the north and northeast, the Cleveland Shale interfingers laterally with the gray Chagrin Shale, a unit that represents prograding prodeltaic deposits of the Catskill clastic wedge (Roen and Kepferle, 1993). Evidence of sediment reworking by storm waves and currents is present in stratigraphically equivalent black shales to the south, in central Tennessee (Schieber, 1994), and to the west, along the crest of the Cincinnati Arch in central Kentucky (McKinsey and Kepferle, 1985). This suggests comparatively shallow water depths in these areas, e.g., a few tens of meters, but the absence of similar features in the four cores of the present study implies deeper water in northern Kentucky and south-central Ohio. Sediment reworking through biotic processes also is minimal in the Cleveland

Shale, which exhibits a low proportion of bioturbated layers (<0.1% of cumulative thickness) compared with the Three Lick Bed and the Huron Member of the Ohio Shale (42% and 7% of cumulative thickness, respectively; Savrda, 1992). This suggests that anoxic conditions existed almost continuously during deposition of the Cleveland Member of the Ohio Shale.

METHODS

Detailed petrographic and geochemical analysis of extended stratigraphic intervals is time-consuming and costly. This problem was overcome in the present study by using X-radiography as the primary tool in analysis of fine-scale compositional variation in laminated cores of the Cleveland Shale. X-radiographs proved useful (1) as a high-resolution proxy record of compositional variation within the study units, (2) as a template for optimal location of samples for petrographic and geochemical analysis, and (3) for construction of continuous gray-scale density (GSD) records for subsequent time series analysis (Fig. 2B). The main procedures used in characterization of the study units included organic petrography, elemental C-S, major- and trace-element, and degree-of-pyritization (DOP) analysis. Different procedures yielded different degrees of stratigraphic resolution: (1) X-radiograph gray-scale density values were measured at equal intervals of 0.02 centimeters over the full length of each study core, (2) geochemical analyses (i.e., C-S, major- and trace-element, and DOP) were undertaken on samples of 0.5-1.0 cm thickness within selected dm-length core intervals, and (3) organic petrographic data were generated for zones of 1.0-2.5 cm thickness from the same core intervals. Correlation coefficients between parameters having different degrees of stratigraphic resolution were calculated using an average value for the parameter of higher resolution over the interval corresponding to a single measurement of the parameter of lower resolution.

X-radiography

Patterns of fine-scale compositional variation in the study cores were initially identified using X-radiography. For a sample of uniform thickness, brightness contrast in X-radiograph images is produced by small compositionally-based differences in rock density such that denser (less dense) areas appear lighter (darker) owing to reduced (increased) X-ray penetration (e.g., Algeo and Woods, 1994; Algeo et al., 1994; Hoffman et al., this volume). In the Cleveland Shale, X-radiograph gray-scale density (GSD; Fig. 2B-C) proved useful as a proxy for organic carbon and sulfide content (Fig. 2D) because the densities of these components (1.0-1.2 and 4.9-5.1 g cm^{-3}, respectively) differ substantially from that of the rock matrix (2.6-2.7 g cm^{-3}), which is composed largely of illite, mixed-layer illite/smectite, other clay minerals, and quartz silt.

Conventional X-radiographic procedures entail cutting samples into thin slabs (commonly <10 mm thick) to minimize interference between sedimentary components and to maximize resolution in the resulting images (e.g., McKinsey and Kepferle, 1985). However, sample slabbing is a time-consuming and fundamentally destructive process and is unnecessary in sedimentary rock cores containing penetrative laminae. This is because high-resolution images can be obtained from moderately thick samples (e.g., 10-50 mm) provided that the X-ray beam is held parallel to sample stratification. In horizontally laminated cores, placement of the core on its side reorients sedimentary laminae vertically, permitting alignment of laminae with a collimated X-ray beam through use of a lead-shielded core stage (Algeo et al., 1994). This approach has several advantages over conventional X-radiographic procedures: (1) higher and more uniform spatial resolution of images, (2) equal exposure of all parts of a sample or core interval, (3) rapidity of analysis (ca. 30 cm hr^{-1}), and (4) non-destructiveness.

For this study, X-radiograph images were produced at the University of Cincinnati using a tungsten-source Hewlett Packard Faxitron (model 43804N) and a custom-built core stage consisting of a platform driven by a variable-speed step motor. Cores were X-rayed in 25-cm-long segments, and each segment was placed on the stage on top of a film holder (containing Kodak Type M film) and covered by a lead shield with a central window of adjustable width. At a source voltage of 60-70 kV, about 5 minutes of exposure was necessary for good image contrast, which was achieved by using a 2.5-cm-wide window and a stage speed of 0.5 cm min^{-1}. Film was developed in Kodak chemicals as specified by the manufacturer, and special attention was paid to film processing to maintain consistent and reproducible results. After development, X-radiograph negatives were scanned at 300 dpi resolution using a UMAC UC630 color scanner and Image-In software and subsequently downloaded to an Optimas image analysis system. In Optimas, line luminance transects were taken along the center of each scanned core segment at a sampling density of 5.3 points per millimeter, providing a continuous record of variation in gray-scale density (GSD) of the core images on a brightness scale ranging from 0 (black) to 255 (white). GSD values were exported to a spreadsheet for further processing, which entailed (1) corrections for non-compositional sources of GSD variance (i.e., minor variations in film exposure and development) using a GSD standard (i.e., a billet with well-defined GSD maxima and minima) and a 2-3-cm overlapping interval between adjacent core segments, and (2) digital splicing of GSD values for successive core segments to produce a continuous GSD data series through the entire Cleveland Shale in each study core (Fig. 2B).

Sampling Procedure

An important preliminary step to petrographic and geochemical characterization of the study unit was selection of sample locations in a manner designed to extract maximum information with reasonable expenditure of effort. A hierarchical sampling strategy was employed with (1) selection of 10-20-cm-long core intervals for detailed sampling in the lower, middle, and upper part of each study unit (e.g., intervals 25/15-16, 22/9-10, and 19/2 in OHRS-5; Fig. 2C), and (2) collection of 19-21 contiguous samples of subequal thickness (0.5-1.0 cm) within each interval of detailed study. Compositional variation exists at several length scales within the Cleveland Shale, and this sampling strategy permitted quantification of petrographic and geochemical parameters at all relevant length scales. Each 10-20-cm-long interval chosen for detailed study enclosed a complete compositional cycle (Fig. 2C), and analysis of 19-21 samples permitted thorough characterization of geochemical changes within each cycle. Analysis of sample sets from the lower, middle, and upper part of each study core was intended primarily to identify secular changes in patterns of compositional variation at a decimeter scale rather than to characterize gross stratigraphic trends in geochemistry, which have been the focus of numerous earlier studies of Appalachian Devonian black shales (e.g., Potter et al., 1980; Robl et al., 1983; Solomon et al., 1984; Leventhal, 1987; Robl and Barron, 1988). Each sample was ground in an agate ball mill, yielding about 6 grams of ca. 400-mesh powder that was split for C-S, major- and trace-element, and DOP analysis. Powdered samples were stored in nitrogen-filled vials and refrigerated to prevent oxidation of organic carbon and sulfides prior to analysis.

Carbon-Sulfur Elemental Analysis

Carbon and sulfur elemental concentrations were obtained on a LECO CS-244 analyzer and induction furnace at Indiana University. About 0.25 g of sample was mixed with iron chips and a chemical accelerator (Lecocel) to promote complete combustion. Multiple analyses of a LECO synthetic carbon standard (reported TC = 5.05 wt%) yielded a mean total carbon value of 5.10±0.19 wt% (n = 43) with a repeatability (intrarun) of ±1.4% to ±2.5% and a reproducibility (interrun) of ±2.0%, yielding an analytical precision (2σ) of ±3.8% of reported values. Carbon and sulfur concentrations were determined on a whole-rock basis for all samples (total carbon, or TC, and total sulfur, or TS; n = 588) and on an acid-volatile-free basis for approximately one in four samples (total organic carbon, or TOC, and non-acid volatile sulfur, or NAVS; n = 149). The latter samples were treated overnight in 2N HCl, and the residues were washed in deionized water and collected on Whatman fiber-glass filters using an aspirator. Inorganic carbon (TIC) and acid-volatile sulfur (AVS) were obtained by difference (cf. Leventhal and Shaw, 1980). A small number of samples will be analyzed for DOP (degree-of-pyritization) using the chromium reduction technique of Canfield et al. (1986), but this analytical step has not been completed yet.

Petrographic Analysis

Petrographic analysis was undertaken on the same 10-20-cm-long core intervals chosen for geochemical analysis, but these were subdivided into a smaller number of zones (n = 7-9 per core interval) of greater thickness (1-3 cm) for the purpose of petrographic point-counts. Zones were chosen on the basis of relatively uniform internal GSD character on the assumption that petrographic variability would be smaller within than between zones. Each core interval was prepared as two or three polished slabs, which were examined using a Carl-Zeiss petrographic microscope under both reflected white light and violet-UV fluorescent light (e.g., Robl et al., 1991). Point-counting was used to determine the relative frequencies of different petrographic components, and observations were made using a 0.3x0.3 mm grid. For each zone, a minimum of 300 observations were collected such that all linear traverses perpendicular to bedding were completed. Organic macerals were classified using standard nomenclature (e.g., Hutton, 1987; Tyson, 1995).

Major- and Trace-Element Analysis

About 3-4 g of each sample were pressed into a pellet and analyzed for whole-rock elemental concentrations using a wavelength-dispersive Rigaku 3040 XRF spectrometer at the University of Cincinnati. Analysis included one run for major and minor elements (Si, Al, Fe, P, Ca, Mg, K, Na, Mn, and Ti) and one for trace elements (Nb, Zr, Y, Cu, Cr, Rb, Sr, Zn, Ni, Ba, Mo, and V). Values for some elements are not reported below owing to (1) concentrations below detection limits (e.g., U) or (2) lack of covariance with other elements (e.g., Na, Mg, Cr). XRF intensities were calibrated using both USGS (SDO-1, SCo-1, SGR-1) and internal black shale standards (analyzed using XRF and INAA by XRAL Incorporated). Analytical precision based on replicate analyses was better than ±1% for Zr, Y, and Rb, ±3.2% for Mn, ±3.8% for Na, ±5% for other trace elements, and ±2% for other major and minor elements. Detection limits for trace elements were 5 ppm for Nb, Zr, Y, Sr, Rb, Zn, Cu, and Ni, 15 ppm for Cr and V, 20 ppm for U, and 50 ppm for Ba.

RESULTS

X-radiography

The gray-scale density (GSD) record of the Cleveland Shale in OHRS-5 exhibits variation at several length scales: (1) for the 18.4-m-thick formation as a whole, GSD values decrease progressively upsection (Fig. 2B), (2) at intermediate length scales (ca. 1-4 m), GSD values vary cyclically and decrease in wavelength upsection (Fig. 2B), and (3) at a fine scale (ca. 0.1-0.3 m), GSD values vary cyclically, also with decreasing wavelength upsection (Fig. 2C). The upsection trend toward lower GSD values reflects primarily an overall increase in organic carbon content toward the top of the Cleveland Shale (e.g., Robl and Barron, 1988), whereas GSD cyclicity at short to intermediate length scales represents stratigraphic variation in the concentrations of both organic carbon and Fe-sulfides (Fig. 2D; see C-S-Fe systematics below). Comparable patterns of variation in GSD values and compositional parameters are present at similar length scales in the other three study cores (Fig. 1; Jaminski et al., 1995).

The three dm-scale compositional cycles in OHRS-5 chosen for detailed analysis display similarities and differences in their GSD records. All three cycles exhibit (1) roughly symmetrical form and (2) greater GSD variability at high GSD values, but (3) lower peak GSD values are observed in interval 22/9-10 than in intervals 19/2 or 25/15-16, and (4) lower background GSD values are present in interval 19/2 than in intervals 22/9-10 or 25/15-16 (Fig. 2C). Within each study core, cycles decrease in thickness upsection (Fig. 2B); however, this thinning appears not to be uniformly distributed within cycles but, rather, to be concentrated within the high-GSD (i.e., low TC-high TS) portions of cycles (cf. intervals 25/15-16 and 19/2, Fig. 2C). GSD variation is largely controlled by total carbon (TC) and total sulfur (TS) concentrations, which are good proxies for the organic carbon and Fe-sulfide content of the samples (see C-S-Fe systematics below). Within the detailed study intervals, (1) TC and TS account for 63% and 64% of total GSD variance, respectively (Fig. 2C-D; n.b., sum >100% owing to TC-TS covariance), and (2) owing to the non-linear response of GSD to variations in TC and TS, GSD covaries more strongly with TC at low to intermediate TC values (Fig. 3A) and more strongly with TS at low to intermediate TS values (Fig. 3B). Strong covariance between GSD values and TC and TS within the dm-scale core intervals chosen for detailed analysis allows GSD to be used as a proxy for TC and TS throughout the study unit.

Carbon-Sulfur-Iron Systematics

In the study area, the Cleveland Shale contains large quantities of organic matter (to 15 wt% TOC) of relatively low rank (R_0 <0.5%, H/C = 0.8-1.4; Maynard, 1981a; Robl et al., 1983; Solomon et al., 1984; Rimmer and Cantrell, 1989). To the east and northeast of the study area, TOC decreases, the proportion of refractory terrestrial organic matter increases, and thermal maturity increases, reflecting (1) greater siliciclastic input in proximity to detrital source areas in the Acadian Orogen to the east, and (2) a higher degree of thermal alteration of organic matter associated with burial in deeper parts of the Appalachian Basin. Stratigraphically, TOC values increase from the base (ca. 4-6%) to the top (ca. 12-14%) of the Cleveland Shale, the upper part of which has been designated a high-grade zone with economic potential as an oil shale (>8% TOC; Robl et al., 1983).

Carbon is present in the Cleveland Shale as organic C and carbonate and sulfur as organic S, sulfides, and sulfates (Robl et al., 1983). However, each of these elements is concentrated dominantly in a single phase, i.e., organic C and pyritic S. In most samples, >80% of total carbon is organic C, and the mean fractional TOC value (i.e., TOC/TC) is 94±9% for the formation as a whole (*n* = 84; Fig. 4A). At least part of the 6% mean difference between TC and TOC is due to incomplete recovery of organic carbon during filtration of acidized samples rather than to presence of carbonate, which is consistent with inorganic C values of <0.2 wt% as determined by CO_2 evolution (Robl and Barron, 1988). In most samples, >75% of total sulfur is non-acid volatile sulfur (NAVS; e.g., Fe-disulfides and organic S), and the mean fractional NAVS value (i.e., NAVS/TS) is 89±10% for the formation as a whole (*n* = 84; Fig. 4B). Although small amounts of acid-volatile sulfur (AVS; e.g., Fe-monosulfides such as greigite and non-Fe-disulfides such as sphalerite) may be present in some samples, loss of NAVS during filtration of acidized samples accounts for at least part of the 11% mean difference between TS and NAVS (Fig. 4B). The relative proportions of Fe-disulfides and organic S in the NAVS fraction were not determined in this study, but organic S concentrations are presumed to be low because (1) petrographic observations demonstrate the abundance of pyrite, (2) negative TOC-TS covariance indicates that most sulfur at low TOC concentrations must be present in non-organic phases, and (3) strong positive Fe-S covariance suggests that both elements are present mainly in Fe-sulfides (see below). Low concentrations of organic S are supported by earlier studies demonstrating that >80% of total sulfur in the Cleveland Shale resides in pyrite (Robl et al., 1983) and that organic S comprises <2 wt% of organic matter extracts (Smith and Young, 1967). For these reasons, we use TS values as a proxy for pyritic S (cf. Lyons and Berner, 1992), which allows a larger number of S determinations to be made.

For the Cleveland Shale as a whole, TC and TS values exhibit moderate negative covariance ($r^2 = 0.21$; $n = 60$; $p(\alpha) < .01$) with a Y-axis intercept of ca. 2.5 wt% TS (Fig. 5A). The three dm-scale cycles chosen for detailed analysis display patterns of TC-TS covariance that are similar in broad outline but differ in detail. Within each cycle, the high TC-low TS interval yielded fairly uniform TC and TS values, representing a stable endpoint, whereas the low TC-high TS interval exhibited continuous variation in TC and TS values, representing an "excursion" from the stable endpoint. However, the paths of TC-TS excursions differ between cycles: (1) in interval 25/15-16, TS increased strongly after TC had already decreased to a minimum (Fig. 5B), (2) in interval 22/9-10, TS increased slightly as TC decreased to a minimum (Fig. 5C), and (3) in interval 19/2, TS first increased and then decreased before the TC minimum was reached (Fig. 5D). In all three cycles, TC-TS excursions were terminated by a decrease in TS, yielding low TC-low TS values, followed by an increase in TC, returning to the stable high TC-low TS endpoint.

Most previous geochemical studies of Devonian black shales from the Appalachian and Illinois basins have inferred either positive C-S covariance or an absence of significant relations. For example, strong positive TOC-TS covariance was observed in the Huron Member of the Ohio Shale and in the Camp Run, Morgan Trail, and lower Clegg Creek members of the New Albany Shale (Robl and Barron, 1988; Ripley et al., 1990; Ingall et al., 1993), similar to patterns observed in modern Black Sea sediments (Lyons and Berner, 1992). On the other hand, little or no TC-TS covariance was observed in the Cleveland Member of the Ohio Shale and in the upper Clegg Creek Member of the New Albany Shale, the upper part of which is correlative with the Cleveland Shale (e.g., Fig. 6; Robl and Barron, 1988; Beier and Hayes, 1989). With the exception of the study by Ingall et al. (1993), which employed a mean sample spacing of 6 cm over a 4.5-m-long core, all of these studies examined thick stratigraphic intervals (25 to >100 m) using low sample densities (ca. 0.5-2.0 m mean spacing). Hence, it is possible that none of these studies have adequately characterized high-frequency patterns of TC-TS covariance (e.g., Fig. 5), which may offer more significant insight regarding controls on organic matter accumulation than low-frequency patterns of TC-TS covariance (e.g., Fig. 6). The results of the present study suggest that high-resolution compositional analysis is essential for understanding environmental conditions and depositional processes within anoxic marine systems.

Strong positive covariation between S and Fe in the Cleveland Shale suggests that both elements reside mainly in Fe-sulfides (Fig. 7), but S:Fe ratios below those of stoichiometric pyrite (2:1) indicate the presence of small quantities of "excess Fe" in other mineral phases. Although monosulfides with a S:Fe ratio of 1:1 would reduce bulk S:Fe ratios, low concentrations of acid-volatile sulfur (Fig. 4B) suggest that little or no monosulfide is present and that excess Fe resides in non-sulfide phases such as clay minerals. Strong positive S-Fe covariance may be an indication that syngenetic sulfide formation in the Cleveland Shale was Fe-limited, because most available reactive Fe is scavenged by sulfides under such conditions (Raiswell and Berner, 1985; Raiswell et al., 1988). Fe-limited conditions are further suggested by (1) weak TC-TS covariance and a positive TS-intercept (Fig. 5; cf. Beier and Hayes, 1989), and (2) generally low TS concentrations (Fig. 6; cf. Robl and Barron, 1988). The definitive test of Fe limitation will be DOP analysis (in progress), but a preliminary evaluation can be made on the basis of Fe-TS relations. If excess Fe mainly resides in reactive phases, then Fe_{total} is a good proxy for $Fe_{pyrite}+Fe_{reactive}$ (i.e., the denominator in DOP calculations) and DOP values can be approximated by Fe_{pyrite}/Fe_{total} (termed DOP_{tot}; Raiswell and Berner, 1985). Mean DOP_{tot} values for the Cleveland Shale are 0.72±0.09 (Fig. 7). Small amounts of monosulfides (≤11% of TS; Fig. 4B) would increase mean DOP_{tot} values to ≤0.80±0.10, whereas small amounts of organic S (≤20% of TS; Robl et al., 1983) would decrease mean DOP_{tot} values to ≥0.58±0.07. Such calculations are tentative but serve to illustrate that DOP values in the Cleveland Shale are likely to be consistent with fully anoxic, Fe-limited conditions (Raiswell et al., 1988). Further, these estimates are similar to DOP values obtained for the Clegg Creek Member of the New Albany Shale (0.6-0.9), the upper part of which is correlative with the Cleveland Member of the Ohio Shale (Anderson et al., 1987; Beier and Hayes, 1989). In samples exhibiting high DOP values, most reactive Fe has been incorporated in Fe-sulfides, and, hence, Fe-sulfide concentrations provide a measure of reactive-Fe flux into such systems (see discussion below).

Petrographic Analysis

The Cleveland Shale is a silty organic-rich shale composed of illite and mixed-layer illite/smectite (45-55%), quartz (25-35%, present in both the silt and clay fractions), organic carbon (5-15%), kaolinite (5%), chlorite (5%), pyrite (5%), and traces of carbonate and feldspar (Robl et al., 1983; Solomon et al., 1984). The main authigenic components are (1) Fe-sulfides, which occur as blebs, stringers, and bands, as well as small (<10 µ) pyrite framboids after greigite(?), and (2) phosphate nodules and diagenetic calcite layers, which are common in some areas but were not observed in the study cores.

Organic matter in the study units includes macerals derived from terrestrial (vitrinite and inertinite) and marine precursors (alginite) and of uncertain origin (bituminite; Robl et al., 1991). Vitrinite and inertinite are present mainly as non-fluorescing detrital fragments (i.e., vitrodetrinite and inertodetrinite); the former are somewhat larger (20-200 µ diameter) and lower in reflectance than the latter. The liptinitic macerals include lamalginite, telalginite, and bituminite. Lamalginite is derived mainly from small (10-100 µ), thin-walled unicellular marine algae, has a distinctive lamellar form with little recognizable internal structure, and exhibits weak to moderate yellow-green fluorescence in samples of low rank. Telalginite is derived from large colonial or thick-walled unicellular algae (e.g., *Tasmanites*, 20-200 µ long) that exhibit distinctive external and internal structures and intense yellow fluorescence in samples of low rank. Alginitic macerals are variably distributed through the sample matrix or concentrated in mm-thick laminae. Bituminite consists of amorphous (i.e., structureless) organic matter exhibiting low reflectance, weak yellow-brown or no fluorescence, and a wispy, disseminated distribution. It is formed through bacterial degradation or secondary gelification of either marine algal or terrestrial humic precursors (Solomon et al., 1984; Taulbee et al., 1990). Although the primary source of bituminite is commonly indeterminate, several observations favor a mainly marine algal precursor in the Cleveland Shale: (1) presence of larger amounts of alginite than of vitrinite and inertinite, even though the latter maceral types are more refractory and, hence, should withstand bacterial degradation better, and (2) positive covariation between the concentrations of alginite and bituminite, and a lack of covariation of either maceral type with vitrinite or inertinite (Fig. 8). A mainly marine algal precursor is also supported by C-isotopic analysis of organic matter in the Cleveland Shale (Maynard, 1981b; Hailer et al., 1983). Bulk organic matter yielded a mean $\delta^{13}C$ value of -28.9±0.6 ‰ PDB (n = 36), which is ^{13}C-depleted in relation to contemporaneous non-marine shales and wood fragments (-25 to -26 ‰). Assuming that the most ^{13}C-depleted samples in distal facies (-30.5 ‰) are representative of the C-isotopic composition of marine organic matter, isotopic mass balance dictates that about 70±10% of the organic carbon in the Cleveland Shale be of marine origin.

Petrographic point-counts revealed systematic variation in organic maceral types at several length scales. Within dm-scale compositional cycles, both alginite and bituminite increase in absolute abundance within high TC-low TS intervals (Fig. 8). However, increases in bituminite are relatively larger than those in alginite, resulting in lower alginite/(alginite+bituminite) ratios. Within the formation as a whole, pronounced stratigraphic trends exist: the relative abundance of alginite decreases upsection from 50-80% to <20% of organic matter whereas that of bituminite increases from 10-40% to >80%, resulting in significantly lower alginite/(alginite+bituminite) ratios (cf. intervals 25/15-16 and 19/2, Fig. 8). Because decreases in alginite/(alginite+bituminite) ratios imply greater bacterial degradation of a marine algal precursor, these trends are consistent with enhanced reworking of organic matter within the high TC-low TS portions of cycles and toward the top of the formation. In contrast, vitrinite and inertinite exhibit relatively low, uniform concentrations (ca. 5-15%) that do not vary in a regular manner either within dm-scale cycles or through the formation as a whole (Fig. 8). This suggests that the flux of terrestrially-derived organic matter was not strongly coupled to the processes controlling compositional variation in the Cleveland Shale.

Major- and Trace-Element Analysis

Major- and trace-element concentrations exhibit strong stratigraphic variation in the Cleveland Shale, with higher concentrations of most trace metals associated with the TOC-enriched "high-grade" zone at the top of the formation (Robl et al., 1983, 1991; Robl and Barron, 1988). Within dm-scale compositional cycles, most elements exhibit strong positive or negative covariance with TC or TS (Fig. 9), suggesting dominant control of bulk sediment geochemistry by processes linked to organic carbon cycling and authigenic Fe-sulfide precipitation. In order to more accurately assess inter-elemental relations, cluster analyses were performed on matrices of Pearson correlation coefficients for element pairs. The results were generally similar for each of the three dm-scale study intervals, revealing four affinity groups: (1) an organic group consisting of C, Mo, V, Ca, and

P, (2) a sulfide group consisting of S, Fe, Cu, and Zn, (3) a detrital group consisting of Ti, Zr, Y, and Nb, and (4) a second detrital group consisting of Al, Sr, Rb, Ba, and K (Fig. 10; cf. Robl et al., 1983). Because Ti and Zr are likely to reside mainly in rutile and zircon grains, the first detrital group probably represents a silt-size clastic fraction with a substantial heavy-mineral component. In contrast, high concentrations of Al and K indicate dominance of the second detrital group by illite, suggesting that it represents the clay-size clastic fraction. Silica does not cluster strongly with any group, probably owing to an association with both the Ti-Zr-rich detrital group (i.e., as quartz silt) and the Al-K-rich detrital group (i.e., in aluminosilicate clay minerals). Although most elements exhibit invariant affinities (i.e., those shown in Fig. 10), a few elements are rather variable in behavior, clustering with different affinity groups in different core intervals or with no group at all (e.g., Ni); these elements may have multiple sources.

For the most part, elemental associations in the Cleveland Shale are similar to those observed in many modern and ancient anoxic marine environments (e.g., Murray et al., 1983; Brumsack, 1986; Bralower and Thierstein, 1987; Ripley et al., 1990; Pratt and Davis, 1992; Murray and Leinen, 1993; Piper, 1994). Mo and V are commonly associated with organic carbon because these elements are reduced to relatively insoluble species that are readily scavenged by organic matter (Lewan and Maynard, 1982; Emerson and Huested, 1991; Breit and Wanty, 1991). The organic association of Ca and P (Fig. 10) suggests that small quantities of phosphate were precipitated upon regeneration of organic phosphorus (Jarvis et al., 1994). Affinity of Cu and Zn with S indicates uptake of these metals in authigenic sulfides (Calvert and Pedersen, 1993), although some fraction of these and other trace metals (e.g., Ni) may have a detrital origin. Association of Rb, Sr, and Ba with the Al-K-rich detrital group is probably due to incorporation of these elements into interlayer cation sites in illite (W. Huff, pers. comm., 1996), whereas association of Nb and Y with the Ti-Zr-rich detrital group is likely to be due to affinity of these elements with heavy minerals (e.g., Murray et al., 1991). Ba is commonly used as a paleoproductivity indicator (e.g., Schmitz, 1987), but weak Ba-TC covariance (Fig. 10) and average Ba concentrations (cf. Turekian and Wedepohl, 1961) imply a lack of much biogenic Ba in the Cleveland Shale. However, Ba is a better paleoproductivity indicator in siliceous than in non-siliceous biogenic deposits (Bishop, 1988) and may not be relevant to primary productivity in the Cleveland Shale environment. In any case, Ba is frequently subject to diagenetic remobilization, as in Middle Devonian shales of the Appalachian Basin (Nuelle and Shelton, 1986).

The two detrital components present in the Cleveland Shale exhibit different affinities: the Ti-Zr-rich component is more closely aligned with the organic group and the Al-K-rich component with the sulfide group (Fig. 10). Although a close stratigraphic relationship is apparent between the Ti-Zr-rich detrital component and the high TC-low TS portions of dm-scale cycles (Fig. 9, top), the association between the Al-K-rich detrital component and the low TC-high TS portions of cycles is less fixed (Fig. 9, bottom). In core interval 19/2, the organic-poor hemicycle consists of a low TC-high TS (sulfide-rich) layer at 5-8 cm overlain by an Al-K-rich (clay-rich) layer at 7-15 cm that contains low concentrations of both TC and TS. Concentration of sulfides within a thin zone in the organic-poor, clay-rich portion of dm-scale cycles is common in the Cleveland Shale, although the stratigraphic position of the sulfide-rich zone is somewhat variable between cycles.

Relations of the detrital components to organics and sulfides were further investigated by cross-plotting detrital element indices versus TC and TS (Fig. 11). The detrital element indices employed were concentration ratios between elements belonging to the Ti-Zr-rich and Al-K-rich groups, e.g., Zr/Al, such that a higher (lower) ratio indicated an increase (decrease) in the Ti-Zr-bearing component relative to the Al-K-bearing component. In all dm-scale study intervals, Zr/Al ratios were correlated positively with TC and negatively with TS, but the relative strengths of these correlations varied between study intervals: e.g., Zr/Al ratios covaried more strongly with TS than TC in interval 19/2 (r^2 = 0.84 vs. 0.61; Fig. 11A) but more strongly with TC than TS in interval 22/9-10 (r^2 = 0.86 vs. 0.43; Fig. 11B). These patterns suggest that (1) the silt-size clastic fraction (i.e., the Ti-Zr-rich detrital component) is preferentially associated with organics, (2) the clay-size clastic fraction (i.e., the Al-K-rich detrital component) is preferentially associated with Fe-sulfides (cf. Lapp and Balzer, 1993), and (3) the relative fluxes of the two detrital components are closely linked to processes controlling organic matter accumulation and authigenic Fe-sulfide formation.

DISCUSSION

Models for genesis of dm-scale compositional cyclicity in the Cleveland Shale must satisfactorily account for observed patterns of covariation among major sediment components (summarized in Table 1). In many cases, such patterns can provide constraints on the relative fluxes of organic and detrital components, sulfate reduction rates, and bulk sedimentation rates, as well as insights on controls on authigenic Fe-sulfide formation and organic carbon accumulation. Existing data for the study units are sufficient to constrain some but not all of these parameters.

The stratigraphic division of dm-scale cycles in the Cleveland Shale into silty organic-rich and clayey sulfide-rich layers is probably due to a combination of depositional and early diagenetic controls (Fig. 12A). Because organic and detrital components are largely immobile in the diagenetic environment, the present alternation of organic-rich and clay-rich layers must reflect primary depositional processes, i.e., a dilution process involving cyclic variation in the flux of organics, clays, or both components, to the sediment (Fig. 12B-C). On the other hand, Fe-sulfides form mainly during early diagenesis in the shallow subsurface environment as a consequence of (1) production of H_2S through bacterial reduction of dissolved sulfate in sediment porewaters, and (2) availability of reactive iron, mainly as Fe-oxyhydroxide coatings on clastic grains (Berner, 1984). With regard to authigenic Fe-sulfide production in the study units, two observations are significant: (1) alginite/(alginite+bituminite) ratios decrease within high TC-low TS intervals (Fig. 8), implying greater bacterial reworking of organic matter and, hence, higher rates of sulfate reduction and H_2S production within organic-rich layers, and (2) sulfide-rich layers occur as relatively thin zones that are commonly located at the contact between underlying organic-rich and overlying clayey layers (e.g., Fig. 9). Because H_2S liberated through sulfate reduction diffuses upward until it is either fixed as a metallic sulfide or becomes oxidized (Berner, 1984), the latter observation suggests that (1) sulfide-rich zones represent the interface along which upward-diffusing H_2S came into contact with reactive Fe, which was present in higher concentrations in the clay-rich layers than in the organic-rich layers (Fig. 12A; cf. Lapp and Balzer, 1993; Shaw et al., 1994), and (2) the distribution of clay-rich layers determined the locus of Fe-sulfide precipitation owing to the existence of Fe-limited conditions (Figs. 6, 7; cf. Canfield, 1989).

An important consideration is whether the dilution process discussed above represented variation primarily in organic carbon rain rates (e.g., related to primary productivity) or in clay-size clastic flux. These alternatives have different implications for bulk sedimentation rates within Cleveland Shale cycles, because a variable organic flux in combination with a constant clastic flux would necessitate higher bulk sedimentation rates within high-TC intervals, whereas a variable clastic flux in combination with a constant organic flux would necessitate higher bulk sedimentation rates within low-TC intervals (cf. Mangini and Dominik, 1979; Kuehl et al., 1993; Arthur et al., 1994). Existing data from the Cleveland Shale favor the latter scenario for the following reason.

High-TC intervals are characterized by lower alginite/(alginite+bituminite) ratios that imply enhanced bacterial reworking of organic matter (Fig. 8). Because concentrations of vitrinite and inertinite are uniformly low within dm-scale cycles, variation in the degree of bacterial reworking of sedimentary organic matter is unlikely to have been due to fluctuations in the supply of labile marine versus refractory terrestrial organics (cf. Berner, 1984; Tyson, 1995). Rather, such variation must have been controlled by some other environmental parameter, e.g., bottomwater oxygen levels or sedimentation rates (cf. Shaw et al., 1994; Kuehl et al., 1993). A redox control is not likely owing to lack of evidence for variation in bottomwater oxygen levels: (1) dm-scale cycles are ubiquitously laminated, consistent with uniformly anoxic conditions (<0.2 ml O_2 l^{-1} H_2O; Wignall, 1994), and (2) concentrations of trace elements sensitive to redox conditions (e.g., Mo and V) vary in roughly constant proportion to organic carbon (Fig. 9). A more likely control on the degree of bacterial reworking of organic matter is sedimentation rate: slow accumulation promotes greater bacterial reworking of organic matter (Canfield, 1994) and, hence, high-TC intervals in the study units containing strongly degraded organic matter were probably deposited at low bulk sedimentation rates (Fig. 13). This inference implies a dilution process governed largely by variations in the clay-size clastic flux (Fig. 12) but does not comment on whether organic carbon rain rates varied, which is critical to an evaluation of preservation versus productivity controls on organic matter accumulation (cf. Canfield, 1994; Arthur et al., 1994). Resolution of this issue may be possible through analysis of variation in organic carbon $\delta^{13}C$ and Fe-sulfide $\delta^{34}S$ values within dm-scale cycles of the study units, which is a future goal of this project (Fig. 13).

With regard to clastic fluxes, covariance of Fe-sulfides with an Al-K-rich detrital component (Fig. 10; Table 1) suggests co-transport of reactive Fe with the clay-size clastic fraction (cf. Lapp and Balzer, 1993), and association of this fraction with low concentrations of relatively well-preserved marine organic matter (Fig. 8) suggests that a high clay flux was responsible for rapid burial and dilution of organics. In contrast, association of high concentrations of strongly bacterially-reworked organic matter with a Ti-Zr-rich detrital component (Fig. 10; Table 1) suggests enhanced deposition of a silt-size heavy-mineral-bearing clastic fraction at low sedimentation rates. The simplest explanation is that the Ti-Zr-rich component represents a background detrital flux, and that the Al-K-rich component represents a second clastic vector of strongly varying intensity (Fig. 12). Although both clastic components may have been water-borne, several lines of evidence suggest an eolian origin for the Ti-Zr-rich component: (1) association with low bulk sedimentation rates, (2) decoupling from the clay-size clastic fraction, which was probably water-borne and exhibited large variations in flux, and (3) inferred presence of heavy minerals, which are commonly transported as an eolian silt-size fraction (cf. Rea et al., 1985; Chuey et al., 1987).

The patterns of covariation among major sediment parameters discussed above provide significant constraints on environmental conditions and processes during deposition of the Cleveland Shale. Turbiditic sedimentation was important within the Late Devonian Appalachian Basin owing to a high rate of sediment input from the rising Acadian Orogen to the north and east. Although no evidence for turbiditic bottomflows is present in the study area, it is likely that the clay-size fraction was deposited hemipelagically, e.g., from turbiditic interflows that travelled great distances along a mid-water pycnocline (Algeo and Woods, 1994). As fluvial discharge and sediment flux generally covary (Nash, 1994), increases in clastic input must have been accompanied by increases in freshwater influx (Fig. 12B). The effect of freshwater plumes is generally to depress and strengthen the pycnocline (Wright, 1977; Garvine, 1984), reducing upward mixing of nutrient-rich deepwaters and potentially lowering surfacewater productivity and organic carbon rain rates. In contrast, low rates of freshwater influx (Fig. 12C) would favor a shallower and weaker pycnocline, promoting vertical mixing of deepwater nutrients into the photic zone and potentially increasing surfacewater productivity and organic carbon rain rates (cf. Malone, 1991). Overall, estuarine circulation is inferred within the semi-restricted Late Devonian Appalachian Basin, consistent with high precipitation and runoff in a humid tropical climate.

In this model, covariance between sedimentary organic carbon and Fe-sulfide concentrations (Fig. 5) was controlled by the interaction of two imperfectly coupled parameters, i.e., freshwater runoff and clastic influx. Organic carbon accumulation rates were linked to freshwater runoff via its effects on vertical mixing and surfacewater productivity, whereas precipitation of authigenic Fe-sulfides depended on the supply of reactive Fe and, hence, on the flux of fine-grained clastics. Freshwater runoff and clastic flux are climate-sensitive parameters (Malone, 1991), and, hence, climatic forcing is likely to have been the ultimate cause of secular environmental variability in the Late Devonian Appalachian Basin. A rough estimate of the timescales associated with climatic forcing is possible: given (1) a formation duration of ca. 250(±2x) ky (i.e., about one-half of a Late Devonian conodont zone; Fig. 2A; Woodrow et al., 1988; Ziegler and Sandberg 1990), (2) a formation thickness of 18.4 m (Fig. 2B), and (3) a mean cycle thickness of 15±5 cm (Fig. 2C), dm-scale compositional cycles in the Cleveland Shale had a mean duration of about 2.0±1.5 ky. Although other scenarios may be possible, a depositional model based on weakly-coupled freshwater and terrigenous clastic fluxes accounts fully for observed patterns of compositional variation in the Cleveland Shale (Table 1).

CONCLUSIONS

Dm-scale compositional cyclicity within the Upper Devonian Cleveland Member of the Ohio Shale (central Appalachian Basin) is manifested as variation between a high TC-low TS endmember and a low TC-high TS endmember. High TC-low TS intervals are characterized by (1) higher organic carbon and lower Fe-sulfide content, (2) larger amounts of alginite (marine algal organic matter) and bituminite (a bacterial degradation product), (3) lower alginite/(alginite+bituminite) ratios (indicating greater bacterial reworking of organic matter), and (4) higher concentrations of trace elements associated with organic matter and with a Ti-Zr-rich detrital group (probably a silt-size heavy-mineral-bearing clastic fraction). Low clastic influx and bulk sedimentation rates are inferred for high TC-low TS intervals on the basis of large amounts of poorly-preserved organic matter (reflecting concentration and bacterial reworking) and low rates of formation of Fe-sulfides (reflecting lack of reactive Fe in a Fe-limited system). In contrast, low TC-high TS core intervals exhibit (1) lower organic carbon and higher Fe-sulfide content, (2) reduced amounts of alginite and bituminite, (3) higher alginite/(alginite+bituminite) ratios, and (4) higher conentrations of trace elements associated with Fe-sulfides and with an Al-K-rich detrital group (probably a clay-size clastic fraction). Higher clastic influx and bulk sedimentation rates are inferred for low TC-high TS intervals on the basis of smaller amounts of better-preserved organic matter (reflecting dilution and rapid burial) and higher rates of formation of Fe-sulfides (reflecting greater availability of reactive Fe). Authigenic Fe-sulfides are commonly concentrated near the base of the low-TC interval and may have precipitated along the interface between an underlying organic-rich layer, which exhibited high rates of sulfate reduction and H_2S production, and an overlying clay-rich layer, which contained large amounts of reactive Fe. These observations are consistent with a depositional model invoking organic matter accumulation under starved-basinal conditions in the central Appalachian Basin during the Late Devonian, punctuated by episodic intensification of freshwater runoff and clastic influx via climatic forcing at timescales of a few thousand years.

Microstratigraphic analysis of laminated organic-rich sediments, as in this study, can yield much more detailed information about depositional processes than geochemical surveys undertaken at broad sampling intervals, which may overlook high-frequency compositional variation entirely. Efficient analysis of fine-scale compositional variation over long core intervals is possible using X-radiography as a primary tool. X-radiography permits (1) construction of continuous high-resolution proxy records of compositional variation, (2) identification of natural length scales of compositional variation prior to sampling, and (3) optimal location of samples for petrographic and geochemical characterization of the study unit. Because stronger patterns of inter-elemental covariance are observed for closely-spaced than for widely-spaced samples, high-resolution compositional analysis is essential for accurate characterization of "instantaneous" conditions and short-term changes in anoxic marine environments.

ACKNOWLEDGMENTS

Thanks to Thomas Robl (Center for Applied Energy Research, Lexington, Kentucky) for loan of the KEP-2 and KEP-3 cores, to Scott Brockman (Ohio Geological Survey) for loan of the OHRS-5 and OHDW-1 cores, and to Lisa Pratt (Indiana University) for use of the Leco C-S analyzer. Thanks also to Jürgen Schieber (Univ. of Texas at Arlington) for editorial handling of the manuscript, to Frank Ettensohn (Univ. of Kentucky) for a careful review, and to Roy Kepferle, Darrell Taulbee, Tom Anderson, and Tim Lyons for helpful discussions on aspects of this project. Support for this project was provided by the University of Cincinnati Sedimentology Fund and by Sigma Xi Grants-in-Aid (1994 and 1995) to the senior author.

REFERENCES

ALGEO, T.J., AND WOODS, A.D., 1994, Microstratigraphy of the Lower Mississippian Sunbury Shale: A record of solar-modulated climatic cyclicity: Geology, v. 22, p. 795-798.

ALGEO, T.J., PHILLIPS, M., JAMINSKI, J., AND FENWICK, M., 1994, High-resolution X-radiography of laminated sediment cores: J. Sed. Res., v. A64, p. 665-668.

ANDERSON, T.F., KRUGER, J., AND RAISWELL, R., 1987, C-S-Fe relationships and the isotopic composition of pyrite in the New Albany Shale of the Illinois Basin, U.S.A.: Geochim. Cosmochim. Acta, v. 51, p. 2795-2805.

APLIN, A.C., BISHOP, A.N., CLAYTON, C.J., KEARSLEY, A.T., MOSSMANN, J.-R., PATIENCE, R.L., REES, A.W.G., AND ROWLAND, S.J., 1992, A lamina-scale geochemical and sedimentological study of sediments from the Peru Margin (Site 680, ODP Leg 112), *in* C.P. Summerhayes, W.L. Prell, and K.C. Emeis (Editors), Upwelling Systems: Evolution Since the Early Miocene, Geol. Soc. London Spec. Publ. 64, p. 131-149.

ARTHUR, M.A., DEAN, W.E., NEFF, E.D., HAY, B.J., KING, J., AND JONES, G., 1994, Varve calibrated records of carbonate and organic carbon accumulation over the last 2000 years in the Black Sea: Glob. Biogeochem. Cycles, v. 8, p. 195-217.

BEIER, J.A., AND HAYES, J.M., 1989, Geochemical and isotopic evidence for paleoredox conditions during deposition of the Devonian-Mississippian New Albany Shale, southern Indiana: Geol. Soc. Am. Bull., v. 101, p. 774-782.

BERNER, R.A., 1984, Sedimentary pyrite formation: An update: Geochim. Cosmochim. Acta, v. 48, p. 605-615.

BISHOP, J.K.B., 1988, The barite-opal-organic carbon association in oceanic particulate matter: Nature, v. 332, p. 341-343.

BOND, G., BROECKER, W., LOTTI, R., AND MCMANUS, J., 1992, Abrupt color changes in isotope stage 5 in North Atlantic deep sea cores: Implications for rapid change of climate-driven events, *in* G. Kukla and E. Went (Editors), Start of a Glacial, Proceedings of the Mallorca NATO ARW, NATO ASI Ser. I, v. 3, p. 185-205.

BRALOWER, T.J., AND THIERSTEIN, H.R., 1987, Organic carbon and metal accumulation in Holocene and mid-Cretaceous marine sediments: Paleoceanographic significance, *in* J. Brooks and A. Fleet (Editors), Marine Petroleum Source Rocks, Blackwell, Oxford, p. 345-369.

BREIT, G.N., AND WANTY, R.B., 1991, Vanadium accumulation in carbonaceous rocks: A review of geochemical controls during deposition and diagenesis: Chem. Geol., v. 91, p. 83-97.

BRUMSACK, H.J., 1986, The inorganic geochemistry of Cretaceous black shales (DSDP Leg 41) in comparison to modern upwelling sediments from the Gulf of California, *in* C.P. Summerhayes and N.J. Shackleton (Editors), North Atlantic Palaeoceanography, Geol. Soc. London Spec. Publ. 21, p. 447-462.

CALVERT, S.E., AND PEDERSEN, T.F., 1993, Geochemistry of Recent oxic and anoxic marine sediments: Implications for the geological record: Mar. Geol., v. 113, p. 67-88.

CANFIELD, D.E., 1989, Reactive iron in marine sediments: Geochim. Cosmochim. Acta, v. 53, p. 619-632.

CANFIELD, D.E., 1994, Factors influencing organic carbon preservation in marine sediments: Chem. Geol., v. 114, p. 315-329.

CANFIELD, D.E., RAISWELL, R., WESTRICH, J.T., REAVES, C.M., AND BERNER, R.A., 1986, The use of chromium reduction in the analysis of reduced inorganic sulfur in sediments and shales: Chem. Geol., v. 54, p. 149-155.

CHUEY, J.M., REA, D.K., AND PISIAS, N.G., 1987, Late Pleistocene paleoclimatology of the central equatorial Pacific: A quantitative record of eolian and carbonate deposition: Quat. Res., v. 28, p. 323-339.

CRAFT, J.H., AND BRIDGE, J.S., 1987, Shallow-marine sedimentary processes in the Late Devonian Catskill Sea, New York State: Geol. Soc. Am. Bull., v. 98, p. 338-355.

DE WITT, W., JR., AND ROEN, J.B., 1985, Correlation and geographic extent of some Middle and Upper Devonian and Lower Mississippian black shales in the Appalachian Basin: U.S. Geol. Surv. Bull., v. 1605-A, p. 45-57.

EMERSON, S.R., AND HUESTED, S.S., 1991, Ocean anoxia and the concentrations of molybdenum and vanadium in seawater: Mar. Chem., v. 34, p. 177-196.

ETTENSOHN, F.R., AND ELAM, T.D., 1985, Defining the nature and location of a Late Devonian-Early Mississippian pycnocline in eastern Kentucky: Geol. Soc. Am. Bull., v. 96, p. 1313-1321.

ETTENSOHN, F.R., GOODMAN, P.T., NORBY, R.D., AND SHAW, T.H., 1989, Stratigraphy and biostratigraphy of the Devonian-Mississippian black shales in west-central Kentucky and adjacent parts of Indiana and Tennessee, *in* Proceedings of the 1988 Eastern Oil Shale Symposium, Institute for Mining and Minerals Research, Lexington, Kentucky, p. 237-245.

GARVINE, R.W., 1984, Radial spreading of buoyant surface plumes in coastal waters: J. Geophys. Res., v. 89, p. 1989-1996.

HAILER, J.G., LEININGER, R.K., AND HAYES, J.M., 1983, Marine vs. terrestrial sources and other influences on the carbon isotopic composition of the organic matter in the New Albany Shale, *in* Proceedings of the 1983 Eastern Oil Shale Symposium, Inst. Mining Mineral Research, Lexington, Kentucky, p. 207-213.

HAY, B.J., HONJO, S., KEMPE, S., ITTEKKOT, V.A., DEGENS, E.T., KONUK, T., AND IZDAR, E., 1990, Interannual variability in particle flux in the southwestern Black Sea: Deep-Sea Res., v. 37, p. 911-928.

HERBERT, T.D., AND FISCHER, A.G., 1986, Milankovitch climatic origin of mid-Cretaceous black shale rhythms in central Italy: Nature, v. 321, p. 739-743.

HOFFMAN, D.L., ALGEO, T.J., MAYNARD, J.B., JOACHIMSKI, M.M., HOWER, J.C., AND JAMINSKI, J., 1997, Regional and stratigraphic variation in bottomwater anoxia in offshore core shales of Upper Pennsylvanian cyclothems from the Eastern Midcontinent Shelf (Kansas), U.S.A., *in* J. Schieber (Editor), Recent Progress in Shale Research, Schweizerbart'sche, p. xx-xx.

HUTTON, A.C., 1987, Petrographic classification of oil shales: Internat. J. Coal Geol., v. 8, p. 203-231.

INGALL, E.D., BUSTIN, R.M., AND VAN CAPPELLEN, P., 1993, Influence of water column anoxia on the burial and preservation of carbon and phosphorus in marine shales: Geochim. Cosmochim. Acta, v. 57, p. 303-316.

JAMINSKI, J., ALGEO, T.J., AND HOWER, J.C., 1995, Decimeter-scale cyclicity in the Upper Devonian Ohio Shale (Cleveland Member) and Lower Mississippian Sunbury Shale: Solar- or orbitally-modulated climatic forcing?: Geol. Soc. Am. Annual Meeting, New Orleans, Abstr. Progr., v. 27, p. 410.

JARVIS, I., BURNETT, W.C., NATHAN, Y., AND 9 OTHERS, 1994, Phosphorite geochemistry: State-of-the-art and environmental concerns: Eclog. geol. Helv., v. 87, p. 643-700.

KUEHL, S.A., FUGLSETH, T.J., AND THUNELL, R.C., 1993, Sediment mixing and accumulation rates in the Sulu and South China Seas: Implications for organic carbon preservation in deep-sea environments: Mar. Geol., v. 111, p. 15-35.

LAPP, B., AND BALZER, W., 1993, Early diagenesis of trace metals used as an indicator of past productivity changes in coastal sediments: Geochim. Cosmochim. Acta, v. 57, p. 4639-4652.

LEVENTHAL, J.S., 1981, Pyrolysis gas chromatography-mass spectrometry to characterize organic matter and its relationship to uranium content of Appalachian Devonian black shales: Geochim. Cosmochim. Acta, v. 45, p. 883-889.

LEVENTHAL, J.S., 1987, Carbon and sulfur relationships in Devonian shales from the Appalachian Basin as an indicator of environment of deposition: Am. J. Sci., v. 287, p. 33-49.

LEVENTHAL, J.S., AND SHAW, V.E., 1980, Organic matter in Appalachian Devonian black shale:

I. Comparison of techniques to measure organic carbon, II. Short range organic carbon content variations: J. Sed. Pet., v. 50, p. 77-81.

LEWAN, M.D., AND MAYNARD, J.B., 1982, Factors controlling enrichment of vanadium and nickel in the bitumen of organic sedimentary rocks: Geochim. Cosmochim. Acta, v. 46, p. 2547-2560.

LYONS, T.W., 1991, Upper Holocene sediments of the Black Sea: Summary of Leg 4 box cores (1988 Black Sea Oceanographic Expedition), *in* E. Izdar and J.W. Murray (Editors), Black Sea Oceanography, Kluwer, Dordrecht, p. 401-441.

LYONS, T.W., AND BERNER, R.A., 1992, Carbon-sulfur-iron systematics of the uppermost deep-water sediments of the Black Sea: Chem. Geol., v. 99, p. 1-27.

MALONE, T.C., 1991, River flow, phytoplankton production and oxygen depletion in Chesapeake Bay, *in* R.V. Tyson and T.H. Pearson (Editors), Modern and Ancient Continental Shelf Anoxia, Geol. Soc. London Spec. Publ. 58, p. 83-93.

MANGINI, A., AND DOMINIK, J., 1979, Late Quaternary sapropel on the Mediterranean ridge: U-budget and evidence for low sedimentation rates: Sedim. Geol., v. 23, p. 113-125.

MAYNARD, J.B., 1981a, Some geochemical properties of the Devonian-Mississippian shale sequence, *in* R.C. Kepferle and J.B. Roen (Editors), Chattanooga and Ohio Shales of the Southern Appalachians (Fieldtrip #3), Geol. Soc. Am. Annual Meeting, Cincinnati, Fieldtrip Guidebooks, v. 2, p. 336-343.

MAYNARD, J.B., 1981b, Carbon isotopes as indicators of dispersal patterns in Devonian-Mississippian shales of the Appalachian Basin: Geology, v. 9, p. 262-265.

MCKINSEY, T.R., AND KEPFERLE, R.C., 1985, X-radiography of the New Albany and Chattanooga Shales (Devonian) along the western flank of the Cincinnati Arch in Kentucky, *in* Proceedings of the 1985 Eastern Oil Shale Symposium, Institute for Mining and Minerals Research, Lexington, Kentucky, p. 261-267.

MURRAY, J.W., SPELL, B., AND PAUL, B., 1983, The contrasting geochemistry of manganese and chromium in the eastern tropical Pacific Ocean, *in* C.S. Wong, et al. (Editors), Trace Metals in Sea Water, NATO Conf. Ser. Mar. Sci. IV-9, Plenum, New York, p. 643-669.

MURRAY, R.W., BUCHHOLTZ TEN BRINK, M.R., GERLACH, D.C., RUSS, G.P., III, AND JONES, D.L., 1991, Rare earth, major, and trace elements in chert from the Franciscan Complex and Monterey Group, California: Assessing REE sources to fine-grained marine sediments: Geochim. Cosmochim. Acta, v. 55, p. 1875-1895.

MURRAY, R.W., AND LEINEN, M., 1993, Chemical transport to the seafloor of the equatorial Pacific Ocean across a latitudinal transect at 135°W: Tracking sedimentary major, trace, and rare earth element fluxes at the Equator and the Intertropical Convergence Zone: Geochim. Cosmochim. Acta, v. 57, p. 4141-4163.

NASH, D.B., 1994, Effective sediment-transporting discharge from magnitude-frequency analysis: J. Geol., v. 102, p. 79-95.

NUELLE, L.M., AND SHELTON, K.L., 1986, Geologic and geochemical evidence of possible bedded barite deposits in Devonian rocks of the Valley and Ridge Province, Appalachian Mountains: Econ. Geol., v. 81, p. 1408-1430.

PASHIN, J.C., AND ETTENSOHN, F.R., 1995, Reevaluation of the Bedford-Berea Sequence in Ohio and Adjacent States: Forced Regression in a Foreland Basin, Geol. Soc. Am. Spec. Paper 298, 68 pp.

PETERSON, L.C., OVERPECK, J.T., KIPP, N.G., AND IMBRIE, J., 1991, A high-resolution Late Quaternary upwelling record from the anoxic Cariaco Basin, Venezuela: Paleoceanography, v. 6, p. 99-119.

PIPER, D.Z., 1994, Seawater as the source of minor elements in black shales, phosphorites and other sedimentary rocks: Chem. Geol., v. 114, p. 95-114.

POTTER, P.E., MAYNARD, J.B., AND PRYOR, W.A., 1980, Final report of special geological, geochemical, and petrological studies of the Devonian shales in the Appalachian Basin. Dept. of Energy, Eastern Gas Shales Project Contract DE-AC21-76MCO5201, 86 pp.

POTTER, P.E., MAYNARD, J.B., AND PRYOR, W.A., 1982, Appalachian gas-bearing Devonian shales: Statements and discussion: Oil and Gas Journal, v. 80, p. 290-316.

PRATT, L.M., AND DAVIS, C.L., 1992, Intertwined fates of metals, sulfur, and organic carbon in black shales, *in* L.M. Pratt, J.B. Comer, and S.C. Brassell, Geochemistry of Organic Matter in Sediments and Sedimentary Rocks, Soc. Econ. Paleontol. Mineral. Short Course Notes 27, p. 1-27.

RAISWELL, R., AND BERNER, R.A., 1985, Pyrite formation in euxinic and semi-euxinic sediments: Am. J. Sci., v. 285, p. 710-724.

RAISWELL, R., BUCKLEY, F., BERNER, R.A., AND ANDERSON, F.T., 1988, Degree of pyritization of iron as a paleoenvironmental indicator of bottom water oxygenation: J. Sed. Pet., v. 58, p. 812-819.

REA, D.K., LEINEN, M., AND JANACEK, T.R., 1985, A geologic approach to the long-term history of atmospheric circulation: Science, v. 227, p. 721-725.

RIMMER, S.M., AND CANTRELL, D.J., 1989, Organic maturation of the Cleveland Member of the Ohio Shale (eastern Kentucky), *in* Proceedings of the 1988 Eastern Oil Shale Symposium, Institute for Mining and Minerals Research, Lexington, Kentucky, p. 401-410.

RIPEPE, M., ROBERTS, L.T., AND FISCHER, A.G., 1991, ENSO and sunspot cycles in varved Eocene oil shales from image analysis: J. Sed. Pet., v. 61, p. 1155-1163.

RIPLEY, E.M., SHAFFER, N.R., AND GILSTRAP, M.S., 1990, Distribution and geochemical characteristics of metal enrichment in the New Albany Shale (Devonian-Mississippian), Indiana: Econ. Geol., v. 85, p. 1790-1807.

ROBL, T.L., AND BARRON, L.S., 1988, The geochemistry of Devonian black shales in central Kentucky and its relationship to inter-basinal correlation and depositional environment, *in* N.J. McMillan, A.J. Embry, and D.J. Glass (Editors), Devonian of the World, v. 2: Sedimentation: Can. Soc. Petr. Geol. Memoir 14, Calgary, p. 377-392.

ROBL, T.L., BLAND, A.E., KOPPENAAL, D.W., AND BARRON, L.S., 1983, Geochemistry of oil shales in eastern Kentucky, *in* F.P. Miknis, and J.F. McKay, J.F. (Editors), Geochemistry and Chemistry of Oil Shale, American Chemical Society, Washington, D.C., p. 159-180.

ROBL, T.L., RIMMER, S.M., AND BARRON, L.S., 1991, Organic petrography of Mississippian and

Devonian shales in east-central Kentucky, *in* Proceedings of the 1990 Eastern Oil Shale Symposium, Institute for Mining and Minerals Research, Lexington, Kentucky, p. 173-178.

ROEN, J.B., AND KEPFERLE, R.C., eds., 1993, Petroleum geology of the Devonian and Mississippian black shale of eastern North America: U.S. Geol. Surv. Bull., v. 1909.

SAVRDA, C.E., 1992, Character and implications of bioturbated oxygenation-event beds in the Ohio Shale (Kentucky), *in* Proceedings of the 1991 Eastern Oil Shale Symposium, Institute for Mining and Minerals Research, Lexington, Kentucky, p. 392-403.

SCHIEBER, J., 1994, Evidence for high-energy events and shallow-water deposition in the Chattanooga Shale, Devonian, central Tennessee, USA: Sed. Geol., v. 93, p. 193-208.

SCHMITZ, B., 1987, Barium, high productivity, and northward wandering of the Indian continent: Paleoceanography, v. 2, p. 63-77.

SHAW, T.J., SHOLKOVITZ, E.R., AND KLINKHAMMER, G., 1994, Redox dynamics in the Chesapeake Bay: The effect on sediment/water uranium exchange: Geochim. Cosmochim. Acta, v. 58, p. 2985-2995.

SMITH, J.W., AND YOUNG, N.B., 1967, Organic composition of Kentucky's New Albany Shale: Determination and uses: Chem. Geol., v. 2, p. 157-170.

SOLOMON, B.J., HUTTON, A.C., HENSTRIDGE, D.A., AND IVANAC, J.F., 1984, Stratigraphy and organic petrography of Mississippian and Devonian oil shale at the Means Project, east-central Kentucky, *in* Proceedings of the 1984 Eastern Oil Shale Symposium, Institute for Mining and Minerals Research, Lexington, Kentucky, p. 365-392.

TAULBEE, D.N., SEIBERT, E.D., BARRON, L.S., AND ROBL, T.L., 1990, Comparison of maceral group chemistries for a New Albany and an Ohio oil shale kerogen: Energy and Fuels, v. 4, p. 254-263.

TUREKIAN, K.K., AND WEDEPOHL, K., 1961, Distribution of the elements in some major units of the Earth's crust: Geol. Soc. Am. Bull., v. 72, p. 175-191.

TYSON, R.V., 1995, Sedimentary Organic Matter, Chapman & Hall, London, 615 pp.

WIGNALL, P.B., 1994, Black Shales, Clarendon Press, Oxford, 127 pp.

WOODROW, D.L., 1985, Paleogeography, paleoclimate and sedimentary processes of the Late Devonian Catskill Delta, *in* D.L. Woodrow and W.D. Sevon (Editors), The Catskill Delta, Geol. Soc. Am. Spec. Paper 201, p. 51-64.

WOODROW, D.L., DENNISON, J.M., ETTENSOHN, F.R., SEVON, W.T., AND KIRCHGASSER, W.T., 1988, Middle and Upper Devonian stratigraphy and paleogeography of the central and southern Appalachians and eastern Midcontinent, U.S.A., *in* N.J. McMillan, A.J. Embry, and D.J. Glass (Editors), Devonian of the World, v. 1: Regional Syntheses: Can. Soc. Petr. Geol. Memoir 14, Calgary, p. 277-301.

WRIGHT, L.D., 1977, Sediment transport and deposition at river mouths: A synthesis: Geol. Soc. Am. Bull., v. 88, p. 857-868.

ZIEGLER, W., AND SANDBERG, C.A., 1990, The Late Devonian standard conodont zonation: Cour. Forschungsinst. Senckenberg, v. 121, p. 1-115.

TABLE 1

Geochemical and Petrographic Characteristics of Endmember Components of Dm-Scale Cycles

	High TC-Low TS Component	Low TC-High TS Component
X-radiograph gray-scale densities	low	high
Organic carbon concentration	high	low
Fe-sulfide concentration	low	high
Variability in organic carbon and Fe-sulfide concs.	low	high
Organic-group element concs. (Mo, V, P, Ca)	high	low
Sulfide-group element concs. (Fe, Cu, Zn)	low	high
Detrital-group-1 element concs. (Ti, Zr, Nb, Y)	high	low
Detrital-group-2 element concs. (Al, K, Rb, Sr, Ba)	low	high
Marine organic maceral concs. (alginite)	high	low
Terrestrial organic maceral concs. (vitrinite, inertinite)	uncorrel.	uncorrel.
Bacterial organic maceral concs. (bituminite)	high	low
Alginite/(alginite+bituminite) ratios[*]	low	high
Vitrinite/(vitrinite+bituminite) ratios[#]	low	high
Degree-of-pyritization (DOP_{tot}^{+})	low	high

---

[*] Degree of preservation of marine organic matter

[#] Degree of preservation of terrestrial organic matter

[+] Fe_{pyrite}/Fe_{total}; n.b., $Fe_{reactive}$ concentrations not available

FIGURE CAPTIONS

FIG. 1. Locations of the four study cores; star marks the core that is the focus of this report (OHRS-5). Geographic distribution (outcrop and subsurface) of the Cleveland Member of the Ohio Shale in the central Appalachian Basin is shown as a shaded field (from de Witt and Roen, 1985).

FIG. 2. (A) Late Devonian timescale and stratigraphy in central Appalachian Basin (Woodrow et al., 1988). (B) X-radiograph gray-scale density (GSD) record for the complete 18.4-m-thick Cleveland Shale in OHRS-5; $n \approx 96{,}000$ GSD measurements. (C) GSD records for three dm-scale cycles chosen for detailed analysis; $n \approx 720$-840 GSD measurements per core interval. Gray-scale density range is 0-255 brightness units; high (low) values represent denser (less dense) intervals. (D) TC and TS values (wt%) for the three core intervals in C; $n = 19$-21 per interval.

FIG. 3. (A) Total carbon and (B) total sulfur vs. X-radiograph gray-scale density for three dm-scale cycles in Figure 2. All three cycles exhibit similar relations between total carbon (TC) or total sulfur (TS) and gray-scale density (GSD). TC and TS account for 63% and 64% of GSD variance, respectively (n.b., sum >100% owing to covariation between TC and TS). Correlation coefficients are based on best-fit 2nd-order (TC) or 3rd-order (TS) polynomial curves (as illustrated). Note that GSD response to a given concentration of TC or TS depends on operational conditions (i.e., current strength and exposure time), which were adjusted to obtain a broad range of GSD values at the TC and TS concentrations characteristic of the study cores; different shale units are likely to yield different GSD responses.

FIG. 4. (A) Total carbon (TC) vs. total organic carbon (TOC; below) and fractional TOC content (above). (B) Total sulfur (TS) vs. non-acid volatile sulfur (NAVS; below) and fractional NAVS content (above). Diagonal lines in lower half of figure represent constant fractional values between 50% and 100%; mean fractional values ($\pm 1\sigma$) are 94±9% (TOC/TC) and 89±10% (NAVS/TS). Based on analysis of whole-rock and acid-treated sample pairs ($n = 84$).

FIG. 5. TC-TS relations for three dm-scale cycles in Figure 2: (A) all samples, (B) interval 25/15-16, (C) interval 22/9-10, and (D) interval 19/2, which are located in the lower, middle, and upper part of the Cleveland Shale, respectively. Stratigraphic base and top of each core interval are indicated. Note upsection increase in TC and overall negative covariation between TC and TS.

FIG. 6. TC-TS relations in the Cleveland Shale. Shown are average TC-TS values for the three dm-scale cycles in Figures 2 and 5 (solid symbols) and for 16 additional dm-length intervals from the other three study cores (open symbols), as well as a TC-TS field for about 100 samples of the Cleveland Shale from northern Kentucky (Robl and Barron, 1988); the latter analyses were run on homogenized 0.6-1.2-m-long core intervals but yield similar results to the 10-20-cm-long core intervals of the present study. Note (1) the diminished range of TC and TS variation compared with that obtained from sub-cm samples (Fig. 5) and (2) the lack of any well-defined pattern of TC-TS covariance. Normal marine and Black Sea trends from Robl and Barron (1988).

FIG. 7. Total sulfur vs. total Fe for interval 19/2; reported as elemental weight percent (not as oxides). The diagonal lines illustrate stoichiometric S:Fe molar ratios for pyrite (2:1) and monosulfides (1:1) as well as constant DOP_{tot} (degree-of-pyritization) values of 1.0, 0.75, and 0.50. DOP_{tot} values were calculated as Fe_{pyrite}/Fe_{total} and assume that all S resides in Fe-sulfides.

FIG. 8. Total carbon (TC), maceral ratios, and petrographic components for the three core intervals in Figure 2. Note the generally strong covariance of all parameters within these dm-scale cycles. Abbreviations for maceral ratios: B = bituminite, A = alginite, and V = vitrinite; high ratios indicate an increase in well-preserved organic matter of marine algal (alginite) or terrestrial origin (vitrinite) relative to poorly-preserved, bacterially-reworked organic matter (bituminite). Number of samples per interval: 19-21 for TC analyses, 8 for petrographic data.

FIG. 9. Stratigraphic variation in elemental concentrations for interval 19/2; values for major elements in wt%, those for trace elements in ppm (n = 19). Note strong covariance of most elements within dm-scale cycles. Elements are arranged by affinity group as determined through cluster analysis (Fig. 10).

FIG. 10. Dendrogram of elemental relations for interval 19/2 based on R-mode cluster analysis. The distance metric was the Pearson correlation coefficient, and clusters were joined using the weighted pair-group centroid method. The position of the phenon line was chosen (1) to coincide with a similarity coefficient range containing few linkages, and (2) to yield a small number of interpretable elemental affinity groups. Asterisks indicate concentrations based on Leco analysis (C and S) rather than XRF analysis.

FIG. 11. Relation of detrital components to TC and TS in intervals 19/2 (A) and 22/9-10 (B). The detrital element ratio Zr/Al provides a measure of the relative concentrations of Ti-Zr-rich clastics (probable silt-size fraction) and Al-K-rich clastics (probable clay-size fraction). Zr/Al ratios covary positively with TC (r^2 = 0.61-0.86) and negatively with TS (r^2 = 0.43-0.84) in all dm-scale study intervals. Ti/Al ratios (not shown) exhibit the same pattern of covariance with respect to TC and TS but somewhat lower correlation coefficients.

FIG. 12. Depositional model for genesis of compositional cyclicity in the Cleveland Shale. (A) Dm-scale compositional variation; relief shown as in outcrop. (B) Depositional processes for low TC-high TS core intervals. (C) Depositional processes for high TC-low TS core intervals. See text for discussion.

FIG. 13. Predicted patterns of covariation between bulk sedimentation rates, organic carbon rain rates, and bulk organic carbon $\delta^{13}C$ and sulfide $\delta^{34}S$ values for depositional systems in which (A) preservation or (B) productivity factors were the dominant control on sedimentary organic carbon accumulation. The preservation model implies that compositional cyclicity is due solely to dilution effects associated with variable clastic flux, whereas the productivity model implies

control of compositional cyclicity by variation in both clastic flux and organic rain rates. Existing data cannot resolve between these models, but organic carbon $\delta^{13}C$ and sulfide $\delta^{34}S$ data may have potential in this regard. For example, invariant primary productivity rates (A) would induce minimal fluctuations in surfacewater [ΣCO_2] and, hence, in the photosynthetic C-isotopic fractionation factor (ε_P), yielding relatively uniform organic carbon $\delta^{13}C$ values; a constant organic rain rate would result in minimal variation in porewater sulfate reduction rates and, hence, in authigenic Fe-sulfide $\delta^{34}S$ values; inferred dilution effects would be due entirely to large variations in bulk sedimentation rates. In contrast, variable primary productivity rates (B) would induce significant fluctuations in surfacewater [ΣCO_2] and, hence, in the photosynthetic C-isotopic fractionation factor (ε_P), yielding variable organic carbon $\delta^{13}C$ values; a variable rain rate of labile marine organic carbon would result in larger fluctuations in porewater sulfate reduction rates and, hence, in authigenic Fe-sulfide $\delta^{34}S$ values; owing to productivity rate changes, only moderate variations in bulk sedimentation rates would be required to account for inferred dilution effects. Values of all parameters increase to the right; parametric scales are relative and no actual values are implied.

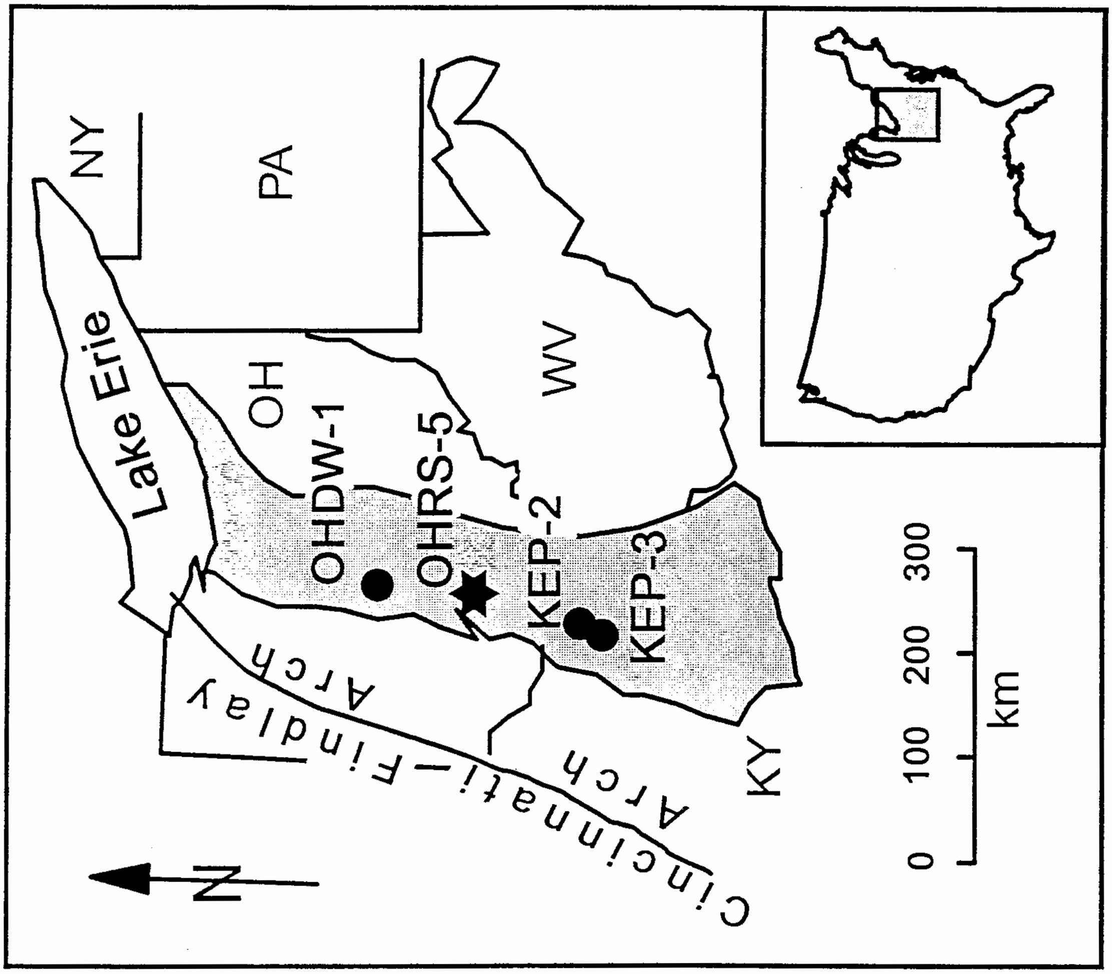
Lake Erie
NY
PA
OH
WV
KY
OHDW-1
OHRS-5
KEP-2
KEP-3
Cincinnati–Findlay Arch
Arch
Arch
N
0
100
200
300
km

FIGURE 1

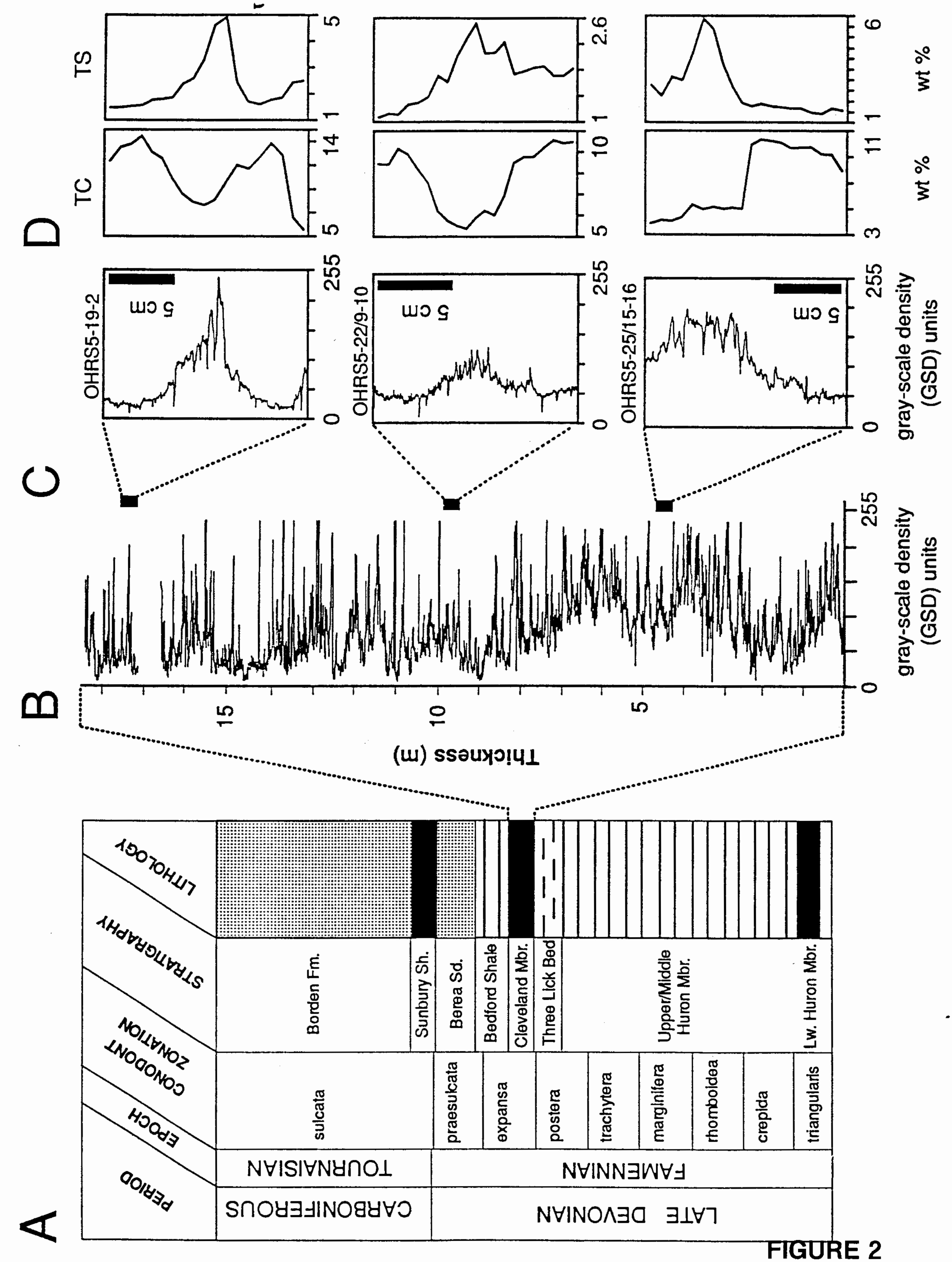
A
PERIOD
EPOCH
CONODONT ZONATION
STRATIGRAPHY
LITHOLOGY
CARBONIFEROUS
LATE DEVONIAN
TOURNAISIAN
FAMENNIAN
sulcata
praesulcata
expansa
postera
trachytera
marginifera
rhomboidea
crepida
triangularis
Borden Fm.
Sunbury Sh.
Berea Sd.
Bedford Shale
Cleveland Mbr.
Three Lick Bed
Upper/Middle Huron Mbr.
Lw. Huron Mbr.
B
Thickness (m)
15
10
5
0
255
gray-scale density (GSD) units
C
OHRS5-19-2
OHRS5-22/9-10
OHRS5-25/15-16
5 cm
0
255
gray-scale density (GSD) units
D
TC
TS
5
14
1
5
10
2.6
3
11
6
wt %
wt %

FIGURE 2

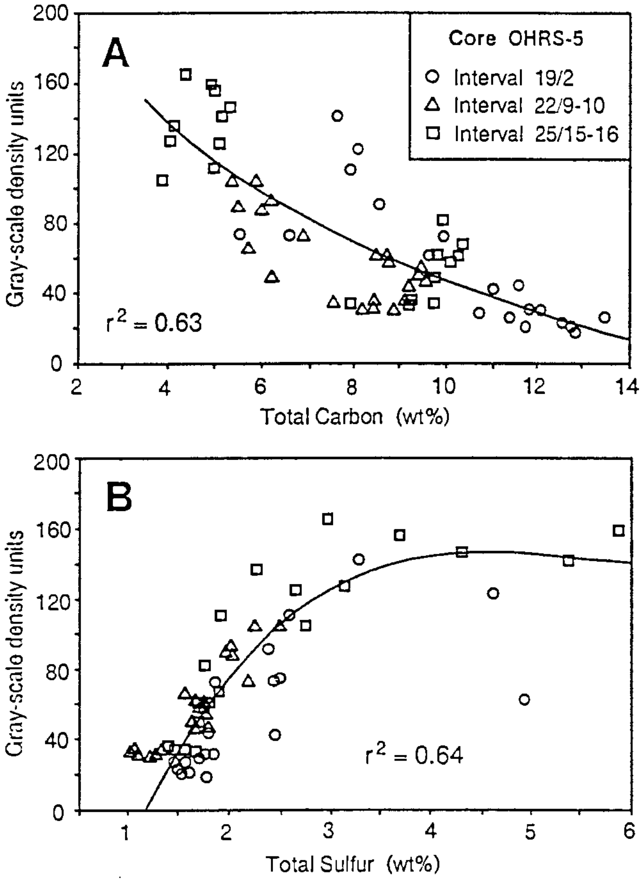
A
Core OHRS-5
○ Interval 19/2
△ Interval 22/9-10
□ Interval 25/15-16
r² = 0.63
Gray-scale density units
0
40
80
120
160
200
2
4
6
8
10
12
14
Total Carbon (wt%)
B
r² = 0.64
Gray-scale density units
0
40
80
120
160
200
1
2
3
4
5
6
Total Sulfur (wt%)

FIGURE 3

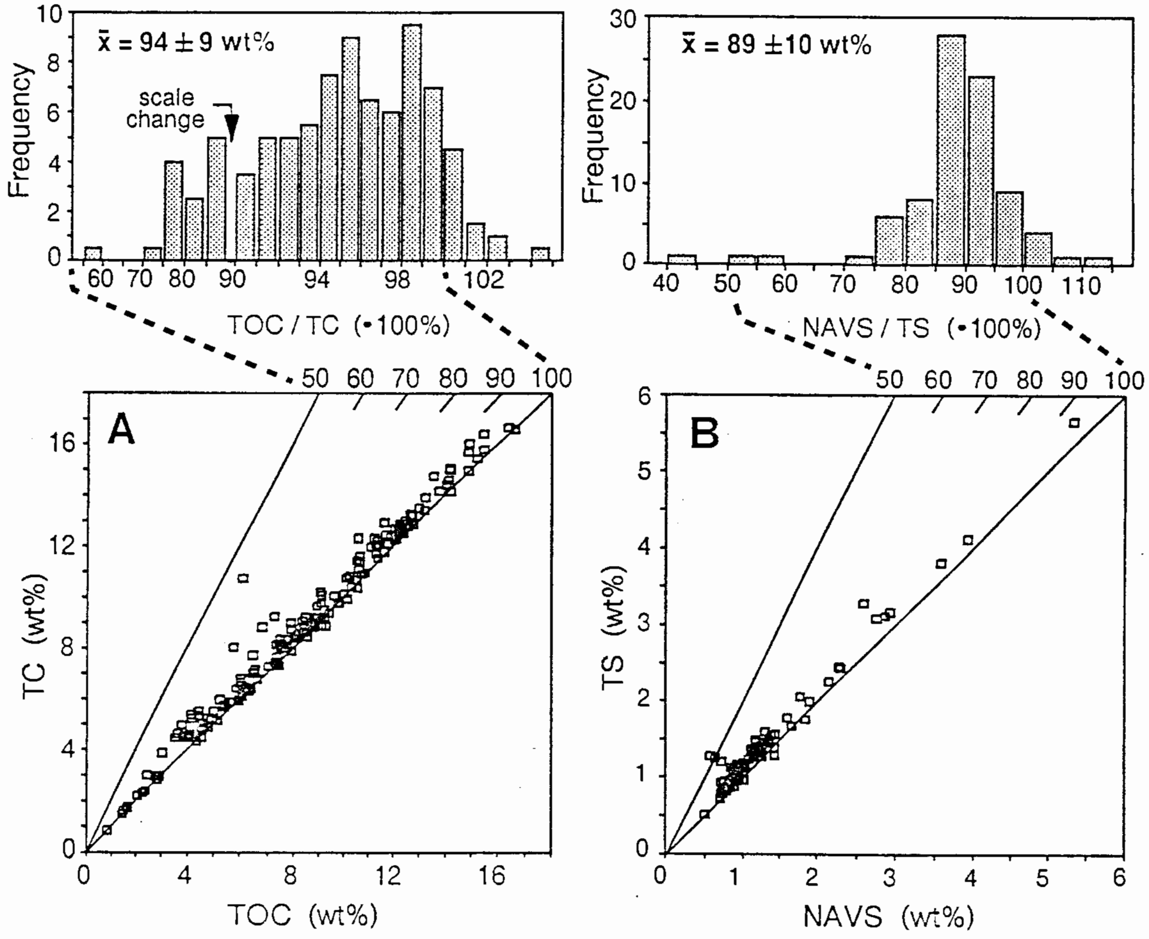
x̄ = 94 ± 9 wt%
Frequency
scale change
10
8
6
4
2
0
60 70 80 90 94 98 102
TOC / TC (•100%)
x̄ = 89 ±10 wt%
Frequency
30
20
10
0
40 50 60 70 80 90 100 110
NAVS / TS (•100%)
50 60 70 80 90 100
A
TC (wt%)
0 4 8 12 16
TOC (wt%)
B
TS (wt%)
0 1 2 3 4 5 6
NAVS (wt%)

FIGURE 4

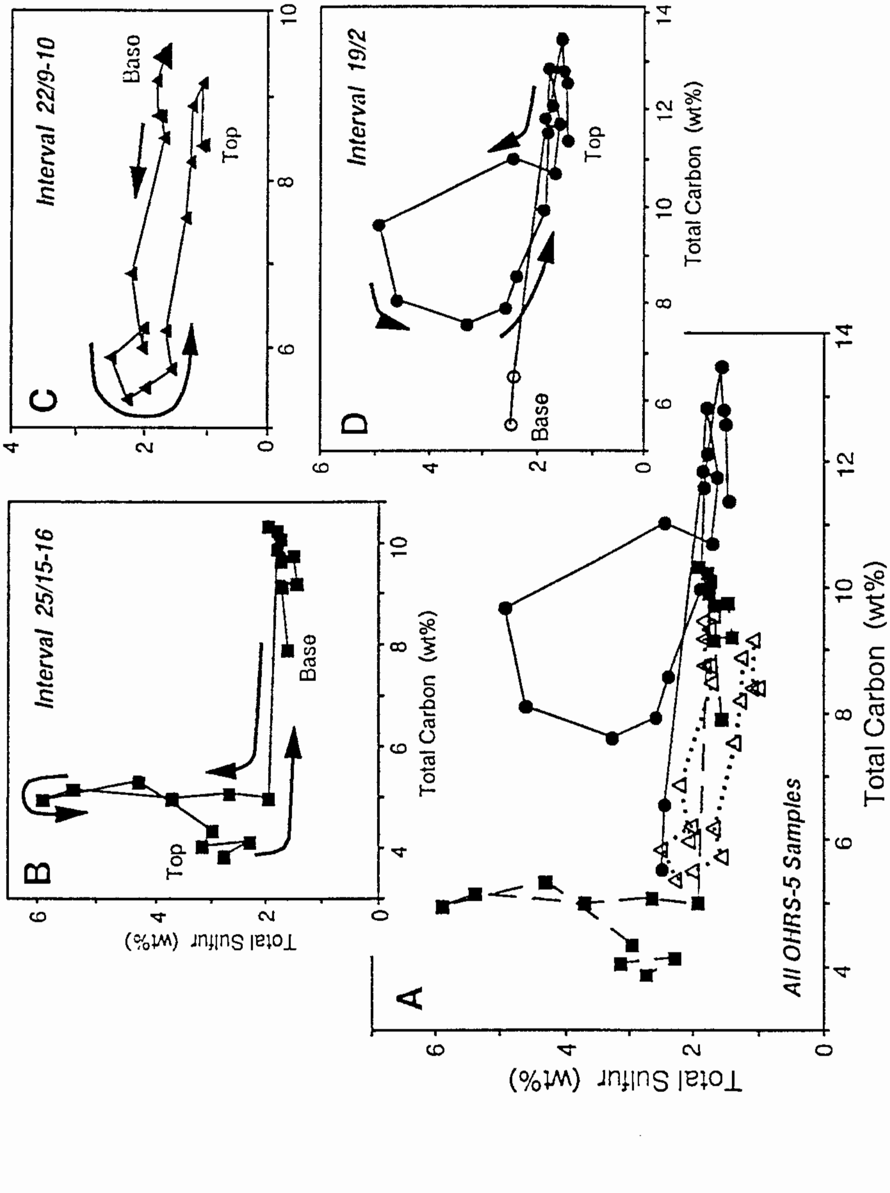
A
All OHRS-5 Samples
Total Sulfur (wt%)
Total Carbon (wt%)
0
2
4
6
4
6
8
10
12
14
B
Interval 25/15-16
Top
Base
Total Sulfur (wt%)
Total Carbon (wt%)
C
Interval 22/9-10
Baso
Top
D
Interval 19/2
Base
Top
Total Carbon (wt%)

FIGURE 5

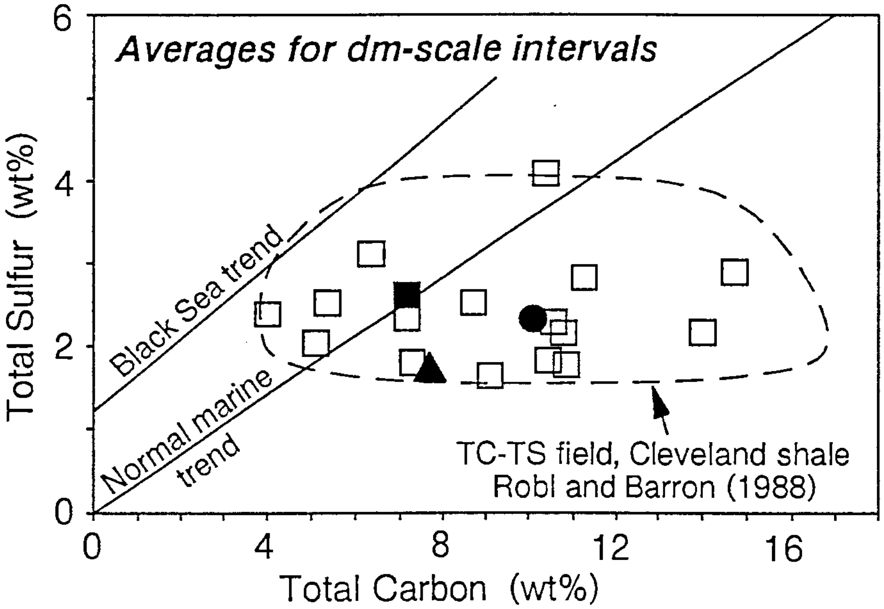
Averages for dm-scale intervals
Black Sea trend
Normal marine trend
TC-TS field, Cleveland shale
Robl and Barron (1988)
Total Sulfur (wt%)
Total Carbon (wt%)
0
2
4
6
0
4
8
12
16

FIGURE 6

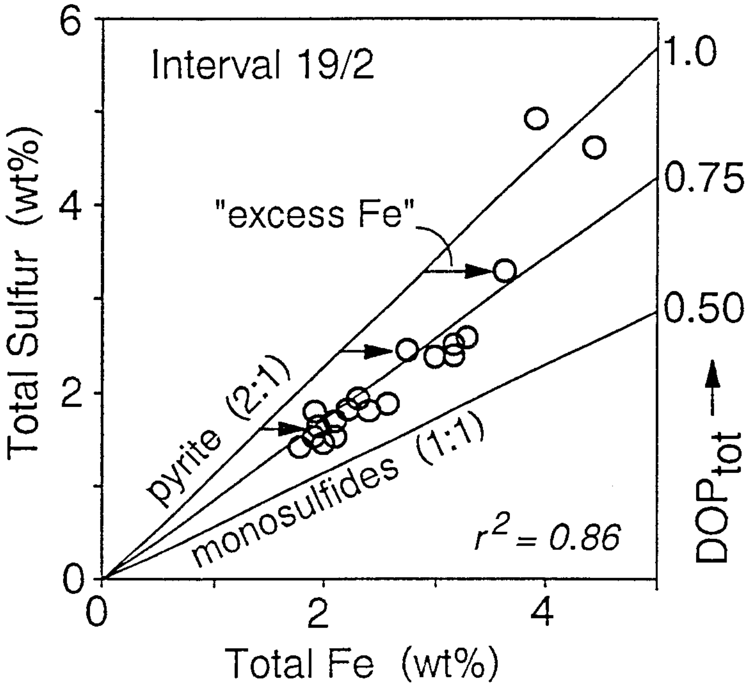
Interval 19/2
"excess Fe"
pyrite (2:1)
monosulfides (1:1)
$r^2 = 0.86$
Total Sulfur (wt%)
Total Fe (wt%)
DOP_{tot}
1.0
0.75
0.50
0
2
4
6
0
2
4

FIGURE 7

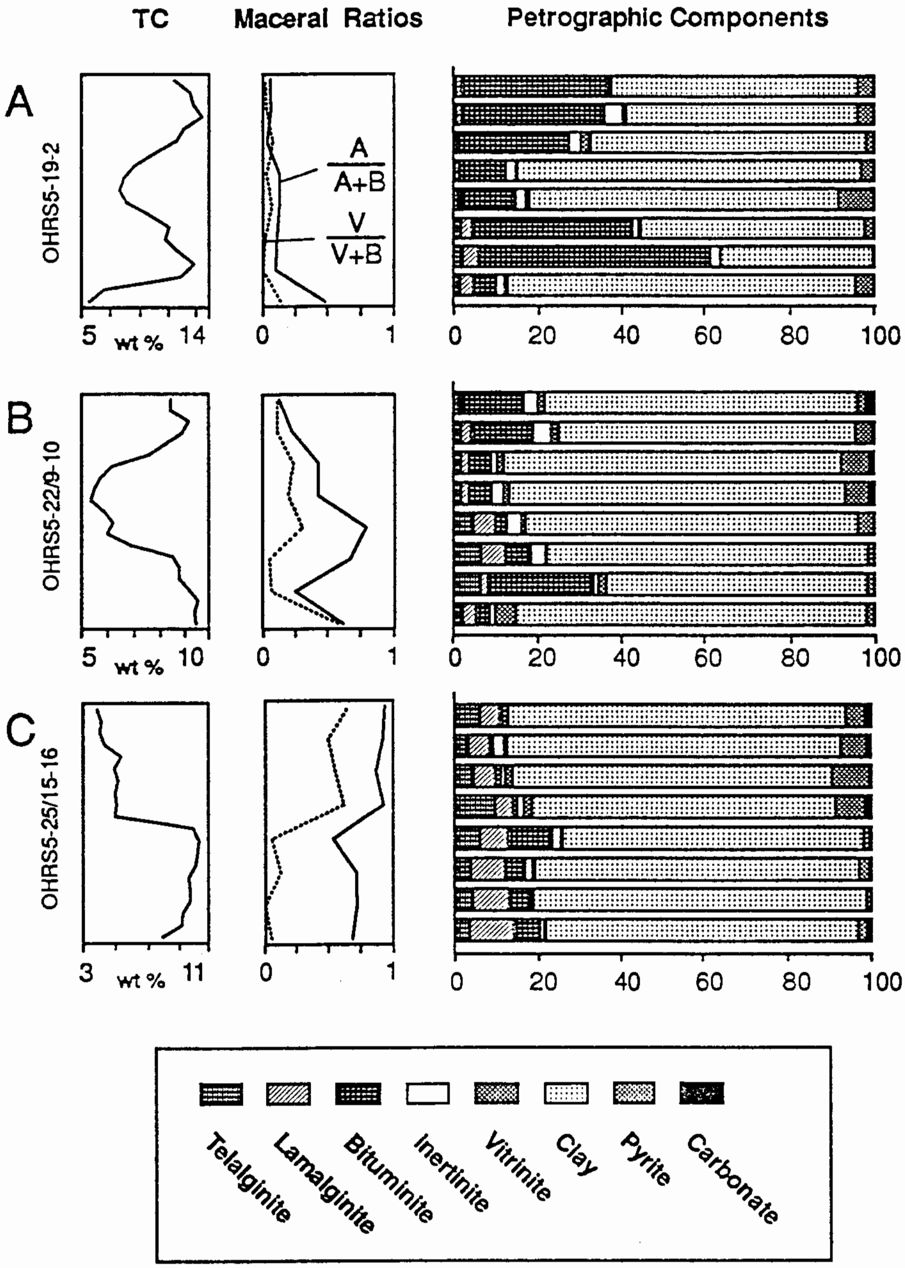
TC
Maceral Ratios
Petrographic Components
A
OHRS5-19-2
A/A+B
V/V+B
5
wt %
14
0
1
0
20
40
60
80
100
B
OHRS5-22/9-10
5
wt %
10
0
1
0
20
40
60
80
100
C
OHRS5-25/15-16
3
wt %
11
0
1
0
20
40
60
80
100
Telalginite
Lamalginite
Bituminite
Inertinite
Vitrinite
Clay
Pyrite
Carbonate

FIGURE 8

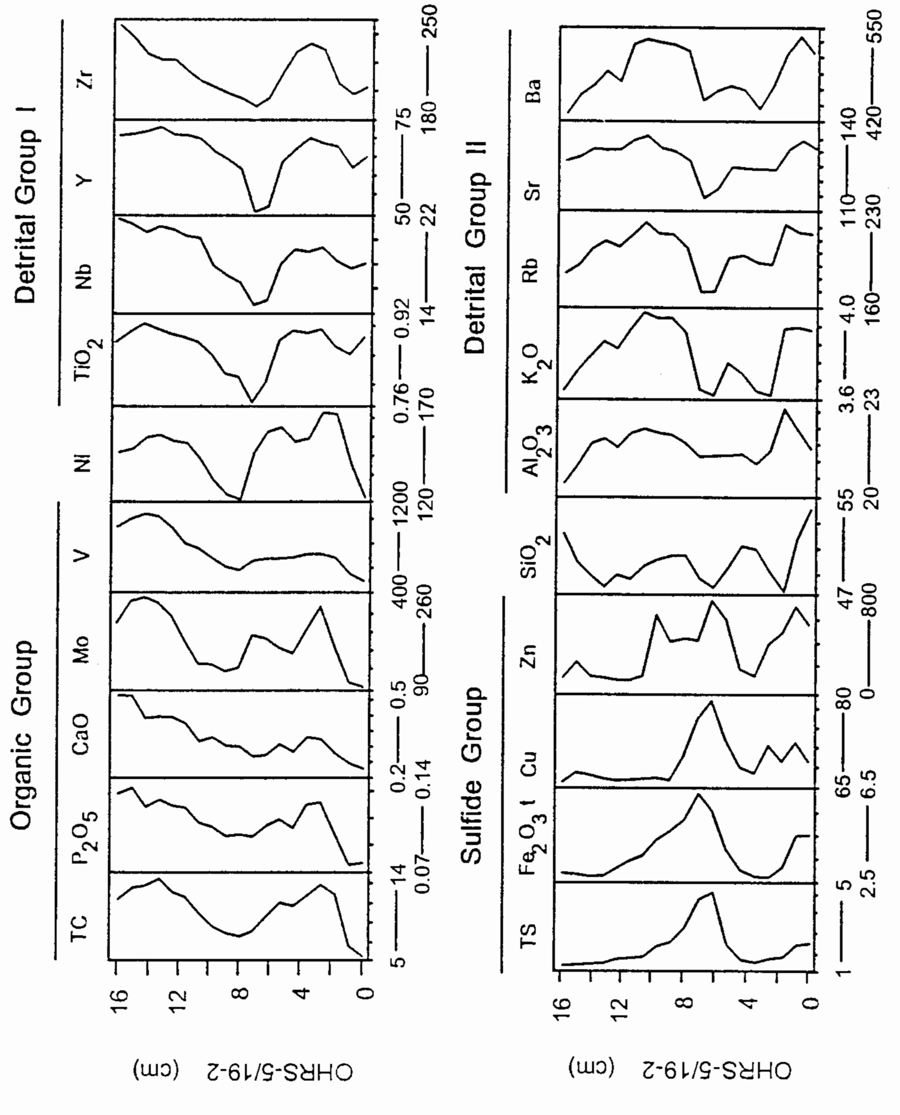
Organic Group
Detrital Group I
TC
P2O5
CaO
Mo
V
Ni
TiO2
Nb
Y
Zr
5 — 14
0.07 — 0.14
0.2 — 0.5
90 — 260
400 — 1200
120 — 170
0.76 — 0.92
14 — 22
50 — 75
180 — 250
16
12
8
4
0
OHRS-5/19-2 (cm)
Sulfide Group
Detrital Group II
TS
Fe2O3 t
Cu
Zn
SiO2
Al2O3
K2O
Rb
Sr
Ba
1 — 5
2.5 — 6.5
65 — 80
0 — 800
47 — 55
20 — 23
3.6 — 4.0
160 — 230
110 — 140
420 — 550
16
12
8
4
0
OHRS-5/19-2 (cm)

FIGURE 9

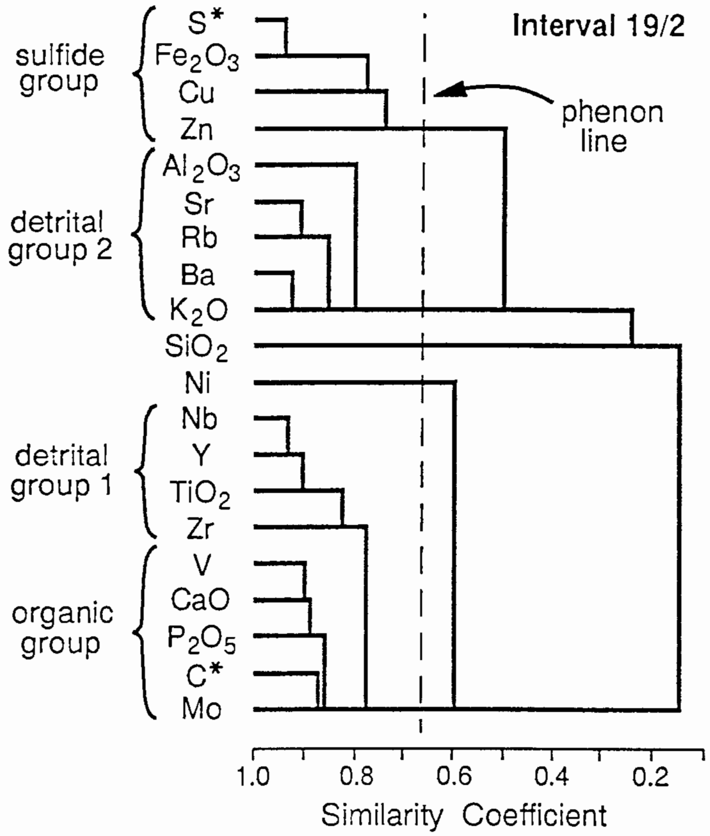
Interval 19/2
sulfide group
S*
Fe2O3
Cu
Zn
detrital group 2
Al2O3
Sr
Rb
Ba
K2O
SiO2
Ni
detrital group 1
Nb
Y
TiO2
Zr
organic group
V
CaO
P2O5
C*
Mo
phenon line
1.0
0.8
0.6
0.4
0.2
Similarity Coefficient

FIGURE 10

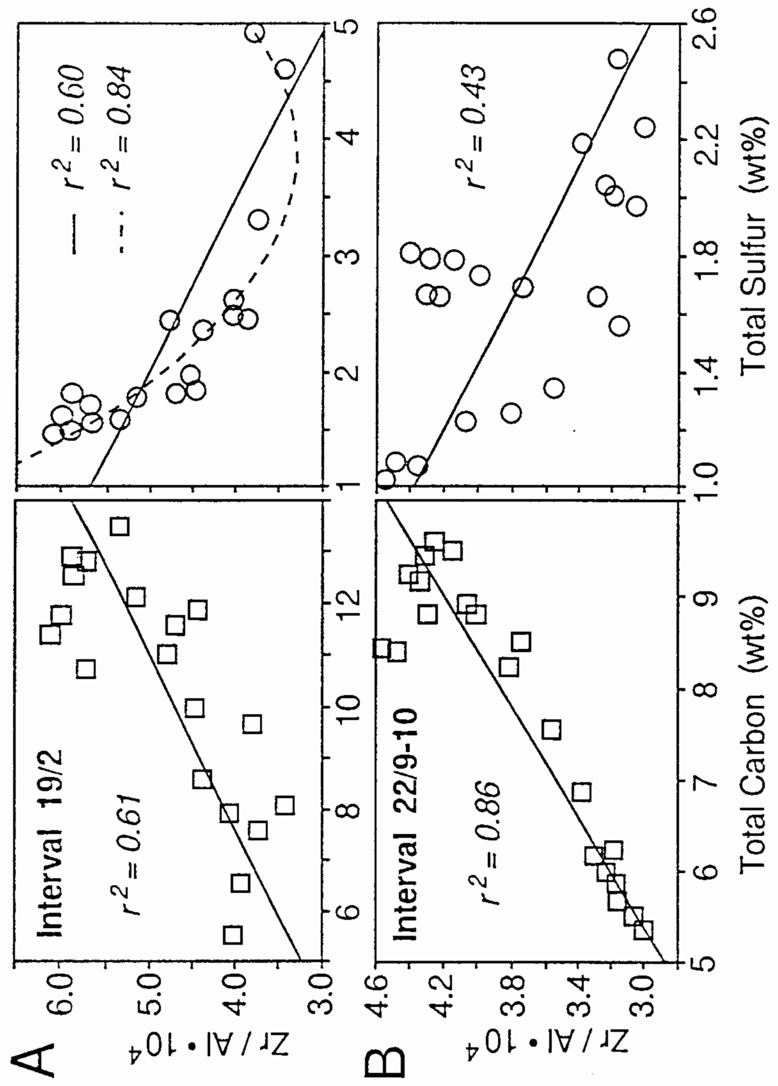
A
Zr / Al • 10^4
6.0
5.0
4.0
3.0
Interval 19/2
$r^2 = 0.61$
6
8
10
12
— $r^2 = 0.60$
- - - $r^2 = 0.84$
1
2
3
4
5
B
Zr / Al • 10^4
4.6
4.2
3.8
3.4
3.0
Interval 22/9-10
$r^2 = 0.86$
5
6
7
8
9
Total Carbon (wt%)
$r^2 = 0.43$
1.0
1.4
1.8
2.2
2.6
Total Sulfur (wt%)

FIGURE 11

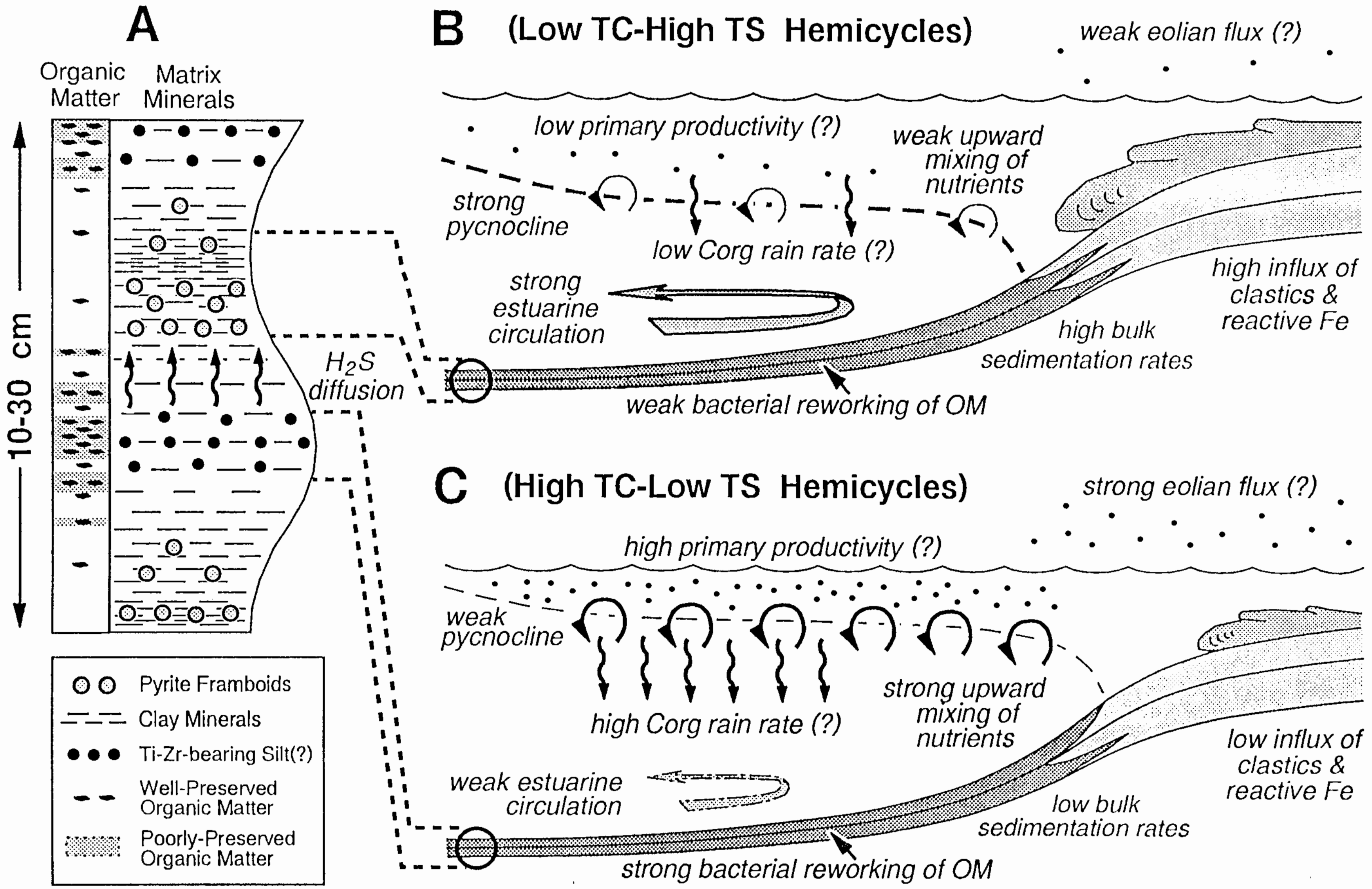
A
Organic Matter
Matrix Minerals
10-30 cm
H_2S diffusion
Pyrite Framboids
Clay Minerals
Ti-Zr-bearing Silt(?)
Well-Preserved Organic Matter
Poorly-Preserved Organic Matter
B (Low TC-High TS Hemicycles)
weak eolian flux (?)
low primary productivity (?)
weak upward mixing of nutrients
strong pycnocline
low Corg rain rate (?)
strong estuarine circulation
high influx of clastics & reactive Fe
high bulk sedimentation rates
weak bacterial reworking of OM
C (High TC-Low TS Hemicycles)
strong eolian flux (?)
high primary productivity (?)
weak pycnocline
strong upward mixing of nutrients
high Corg rain rate (?)
weak estuarine circulation
low influx of clastics & reactive Fe
low bulk sedimentation rates
strong bacterial reworking of OM

FIGURE 12

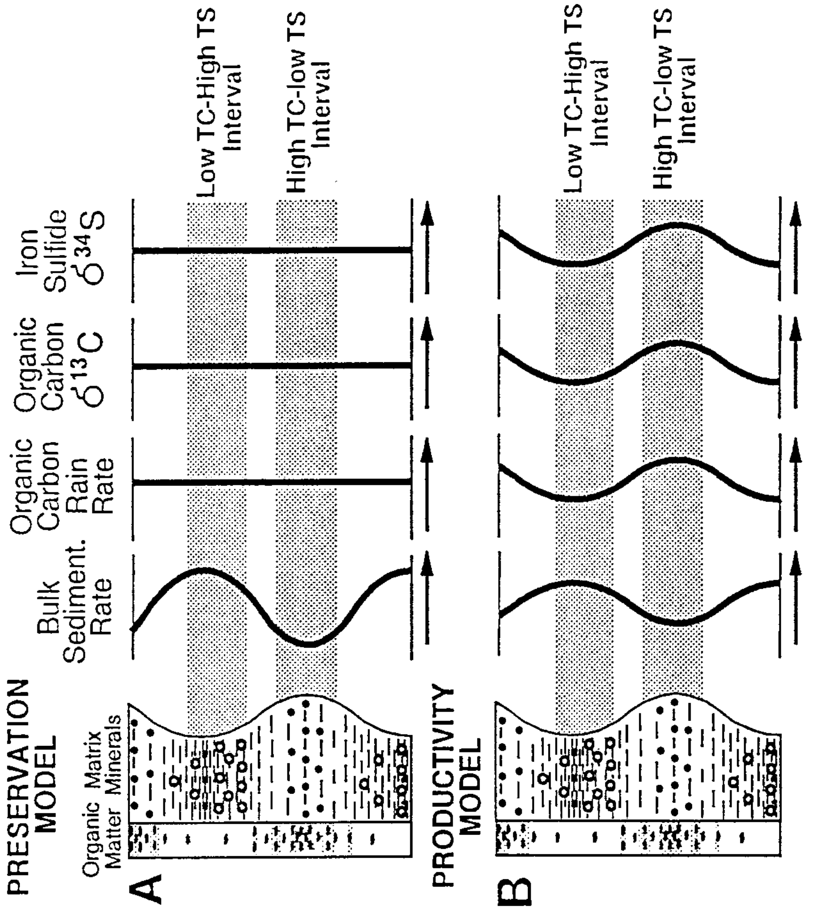
A
PRESERVATION MODEL
Organic Matter
Organic Matrix Minerals
Bulk Sediment. Rate
Organic Carbon Rain Rate
Organic Carbon $\delta^{13}C$
Iron Sulfide $\delta^{34}S$
Low TC-High TS Interval
High TC-low TS Interval
B
PRODUCTIVITY MODEL
Organic Matter
Organic Matrix Minerals
Low TC-High TS Interval
High TC-low TS Interval

FIGURE 13